UNITED NATIONS UNIVERSITY
GEOTHERMAL TRAINING PROGRAMME
Orkustofnun, Grensásvegur 9,
IS-108 Reykjavík, Iceland

Reports 2007
Number 15

THE ISOTOPIC AND CHEMICAL CHARACTERISTICS OF GEOTHERMAL FLUIDS IN HENGILL AREA, SW-ICELAND: HELLISHEIDI, HVERAGERDI AND NESJAVELLIR FIELDS

Marietta W. Mutonga
University of Nairobi
School of Physical and Biological Sciences
Department of Geology
P.O. Box 30197-00100, Nairobi
KENYA
mariettamu@yahoo.com ; mariettamu@gmail.com

ABSTRACT

Results of geochemical and isotopic investigations in the Hengill geothermal area are presented. The area can be regarded as typical of Icelandic high temperature areas. It is mainly composed of pillow lavas and hyaloclastites, which were piled up during sub-glacial eruptions. Part of the area is traversed by a very active NE-SW trending fracture zone about 5 km broad, within which there are several eruptive fissures of postglacial age. The volcanic rocks are basalts of various kinds, but minor occurrences of intermediate and rhyolitic rocks have also been recorded. The study was based on chemical and isotopic analyses of fluid samples from Nesjavellir prior to production, and data collected in the years 2000-2007 from the productive geothermal fields. In addition, fluid samples were collected from the Nesjavellir and Hellisheidi fields during this study. These samples were analysed for chemical constituents and stable isotopes at the Institute of Earth Sciences, University of Iceland.

The results indicate that the Nesjavellir and Hellisheidi thermal fluids do not share the same origin. In Nesjavellir the water comes from a distant source, the glacier Langjökull, whereas in Hellisheidi the water is of a more local origin. The isotopic composition of the thermal waters in Hellisheidi and Hveragerdi is very similar. According to the deuterium isotope values, fluids from well HE-1 in Hellisheidi (Kolvidarhóll-1) are closer in origin to the Nesjavellir thermal fluid than the fluids circulating the Hellisheidi system. It is suggested that the Hellisheidi system is younger than the Nesjavellir system, both by stable isotope and chemical composition of the thermal fluids (Cl-SO_4-HCO_3 plot). In Nesjavellir the fluid is richer in ^{18}O and chemically more mature than in Hellisheidi, due to more intense water-rock interaction. An increase is observed in chloride and enthalpy in both the Nesjavellir and Hellisheidi fields due to increased utilisation. There is a pressure drop in both fields which causes boiling of the liquid phase which results in cooling, and hence a positive temperature gradient is created between the aquifer rock and the flowing fluid. Evidence of boiling is supported in both Nesjavellir and Hellisheidi by high CO_2 values.

1. INTRODUCTION

Iceland is located on the junction of the Mid-Atlantic Ridge and the Greenland-Iceland-Faeroe Ridge, the former being a part of the global mid-oceanic ridge system. Iceland is regarded as being a hot spot above a mantle plume, and has been piled up through emission of volcanic material, created by rifting and crustal accretion through volcanism along the NE-SW axial rift zone. This is sometimes referred to as the neovolcanic zone (Figure 1). Currently, the plume channel reaches the lithosphere below the northwest part of the glacier Vatnajökull. The buoyancy of the Icelandic plume leads to dynamic uplift of the Icelandic plateau, and the high volcanic productivity over the plume produces a thick crust. The western part of Iceland lies west of the volcanic zones and belongs to the North American plate whereas the eastern part of Iceland belongs to the Eurasian plate. As new crust is created along the rift zone, old bedrock moves further from the plate boundary. Therefore, the oldest rocks exposed on the surface in Iceland and formed about 16 million years ago, occur in the easternmost and westernmost parts of the country. The active periods of volcanic systems have been found to vary from 300,000 to over 1 million years. They are preserved as entities in the volcanic pile, indicating that they grew, drifted off towards the margin of the volcanic zone and then became extinct. New ones replaced them over the more or less stationary deep-seated zone of magma generation (Saemundsson, 1967).

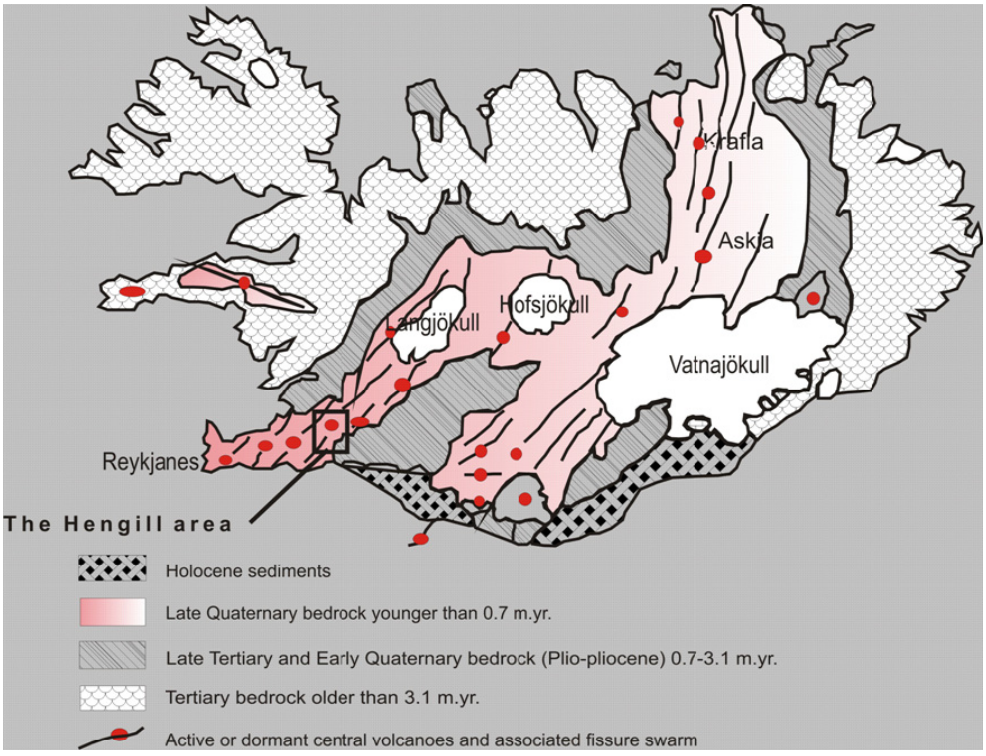

FIGURE 1: The Hengill area in relation to the volcanic rift zone of Iceland and the main rock types (Jóhannesson, H., pers. comm..)

The volcanic zone is connected to the Atlantic ridge across transform faults in both North and South Iceland. In SW-Iceland, the volcanic rift zone is divided into two separate parallel zones characterized by many fissures and fault swarms. The two branches are connected by the E-W trending South Iceland Seismic Zone (Saemundson, 1978). The Hengill area is located just north of a ripple junction where an oblique spreading ridge, tensional spreading axes and a major seismic zone meet.

Geothermal areas in Iceland have been grouped into high-temperature and low-temperature areas (Bödvarsson, 1960; 1961). The high-temperature areas are confined to the active volcanic zones whereas the low-temperature areas are mainly found in the Tertiary and Quaternary rocks. The low-temperature areas are characterised by temperatures below 150°C at 1 km depth, whereas the high-

temperature areas are characterised by temperatures above 200°C at1 km depth. According to this classification, the Hengill geothermal area is a high-temperature area. It is a part of the volcanic rift zone in SW-Iceland, about 40 km east of Reykjavík. The geology is characterized by the active Hengill central volcano, the Hrómundartindur volcanic system and the extinct Hveragerdi volcanic centre hosting geothermal resources. Geology, geophysics, and drilling indicate a total resource area of around 110 km^2 (Gunnlaugsson and Gíslason, 2005). The bedrock in the Hengill area is composed of basaltic lava layers, thick sequences of hyaloclastites, and vertical intrusions. Reservoir fluids are 240-330°C dilute water, low in total dissolved solids (TDS) and gas. The geothermal reservoirs are liquid dominated and temperatures commonly correspond to the boiling-point-with-depth profile.

The Hengill area contains three geothermal fields which are currently being economically exploited for heating water and power production. These are Hellisheidi, Hveragerdi and Nesjavellir (Figure 2). In the Nesjavellir field, northeast of Mt. Hengill, 26 wells have been drilled. The depth of these wells ranges from 1000 to 2200 m and temperatures of up to 380°C have been recorded. The average thermal power from these wells is 60 MWt and 9 MWe. The total power production of the Nesjavellir power plant is 120 MWe and 1640 l/s of water at 83°C (Gíslason et al., 2005). In Hellisheidi, which is to the south of Mt. Hengill, 28 wells have been drilled to date to depths of 2-3 km; 25 of these are deviated wells mainly targeting volcanic fractures and graben boundaries. A power plant has been operating from 2006 in this field producing 90 MWe, and was increased to 120 MWe in late 2007 (Gíslason, G., pers. comm.). Hveragerdi is located some 50 km from Reykjavík and is on the southeast margin of the Hengill geothermal area. Numerous drillholes have been sunk in the area, mainly for space heating and greenhouses. Measured temperatures in this field range from 170 to 240°C.

The harnessing of geothermal heat from the Hengill area has been going on for some decades. Steam and water samples have been taken several times during discharge periods to establish the chemical characteristics of the wells and to monitor any changes (Gíslason, G., pers. comm.). The present study is based on the analysis of fluid samples and on the results of previous work in the exploited geothermal fields. Chemical and isotopic evaluation of geothermal fluids within the Hengill area will be carried out to study if mixing of thermal fluid is taking place, to evaluate chemical characteristics of the thermal fluid, to determine subsurface fluid flow paths, the origin of geothermal fluids and temperature in the Hengill geothermal area and, furthermore to distinguish between and classify the thermal fluids in the fields. In doing so, it is hoped that the data can be used to monitor any possible changes due to production/ exploitation or otherwise, now and in the future. The main emphasis will be on geochemical trends.

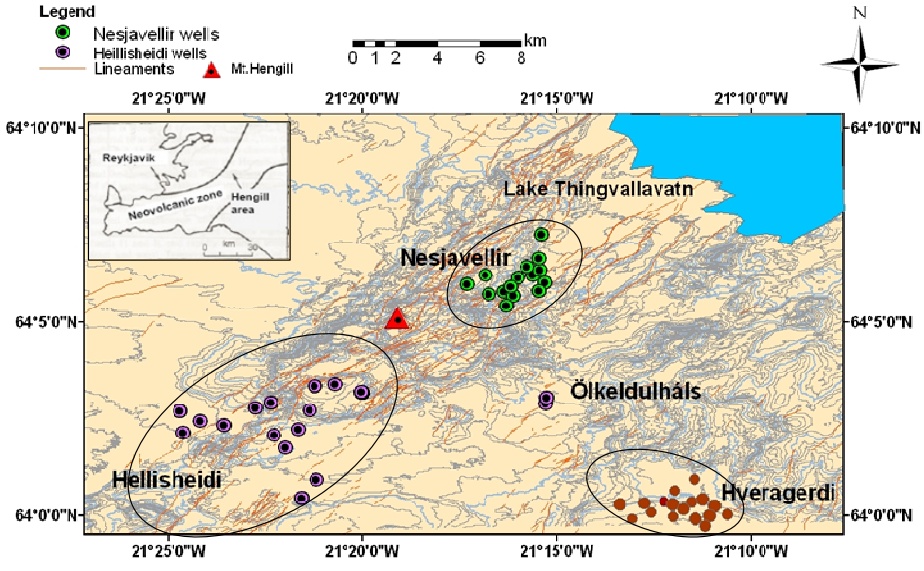

FIGURE 2: Location of the main geothermal fields and wells drilled in the Hengill area

2. GEOLOGICAL SETTINGS

2.1 The Hengill volcano

A great deal of research work has been carried out in the Hengill area by different scientists on its geology, geophysics, geothermal activity and geochemistry. Saemundsson (1967; 1995) mapped the Hengill mountain and produced a 1:25,000 scale geological map. The bedrock in the Hengill area is composed of basaltic lava layers, thick sequences of hyaloclastites, and vertical intrusions.

The Hengill mountain which is also the main expression of the Hengill central volcano rises about 500 m above its surroundings. The fissure swarm is over 50 km long trending N30-35°W and has a structure of a nested graben. Besides the major fissure swarm there are some faults and eruptive fissures transecting the centre of Mt. Hengill in a NW-SE direction towards the Hveragerdi system, i.e. perpendicular to the main tectonic trend. Nearly all high-temperature areas in Iceland are situated within an active central volcano or associated fissure swarm and hence are located in the volcanic rift zone. This indicates that the main heat source must be magmatic intrusions in the upper crust. Two NNE-WSSW striking volcanic fissures, which erupted and intersected the Hengill volcano 2,000 and 5,500 years ago, act as primary conduits for sub-surface fluid flow in both Hellisheidi and Nesjavellir. Normal faulting is extensive and strikes NNE-SSW expressed in a fractured 3–4 km wide graben that has proven highly productive when drilled into. Other fault directions are evident, such as N-S.

The Hengill mountain was mostly accumulated in one or two large sub-glacial eruptions during the last glacial period. Recent geological data suggest that the lower part of the mountain may have formed during the second last glacial period (Fridleifsson, G.Ó., pers. comm.). Hyaloclastite tuft, a typical formation in Iceland, is fine, glassy debris formed by the sudden contact of hot and coherent magma with either cold water or water-saturated sediments, usually associated with glaciers. Rapid heat loss from the magma to the ice sets up tensile thermal stress in the magma carapace as it cools, chills and contracts, causing the glassy, chilled magma to fragment and form quenched fragmented debris. If the deposit remains in contact with water after its formation, the glassy debris may hydrate further to form palagonite. According to Saemundsson (1995), the oldest rocks outcrop in the southeast near the village of Hveragerdi being mostly hyaloclastites overlain by basalt flows, probably pre-dating the last glaciations. Shield volcanoes of last interglacial age are located east and west of Lake Thingvallavatn. Hyalocalstites and pillow lavas forming ridge-shaped mountains, the product of subglacial fissure eruptions, occur to the west and north clearly overlying the oldest layers. These date back from the last glacial period, but may span a wide range within those limits.

The Hengill area is one of the largest high-temperature areas in Iceland, extending over some 50 km^2. The geothermal activity is believed to be connected to three volcanic systems (Figure 3) (Saemundsson, 1995):

1) The Grensdalur system is the oldest and gives heat to the Hveragerdi field;
2) North of this is a volcanic system named after Mt. Hrómundartindur, which last erupted about 10,000 years ago. The geothermal area in Ölkelduháls is connected to that system; and
3) West of these volcanic systems lies the presently active Hengill volcanic system, with intense tectonic activity and NE-SW trending volcanic fractures and faults extending from Lake Thingvallavatn to Nesjavellir and further to the southwest through Innstidalur, Kolvidarhóll, Hveradalur and Hellisheidi (Saemundsson, 1979). The area is almost entirely built up of volcanic rocks of late Quaternary and postglacial age (Saemundsson, 1995). These are mostly basalt flows and hyaloclastites but small amounts of intermediate rocks and rhyolites occur as well.

A seismic study in the Hengill area between 1993 and 1997 registered nearly 24,000 earthquakes exceeding 0.5 on the Richter scale, 12,000 of these occurred in 1997 (Sigmundsson et al., 1997) . The largest earthquake in recent times registered 5.3 on the Richter scale and occurred in June 1998. The

earthquakes seem to have reactivated the geothermal manifestations in the area causing the emergence of new geothermal ones in new areas or the rejuvenation of extinct ones (Natukunda, 2005). From Hengill, there is a lineation of surface manifestations extending southeast from Nesjavellir towards the village of Hveragerdi. It coincides with a low-resistivity anomaly connecting the Hengill area and the extinct Grensdalur central volcano. It shows an anomaly perpendicular to the main fissure swarm and parallel to the transverse lineament in the Hengill system (Björnsson et al., 1986).

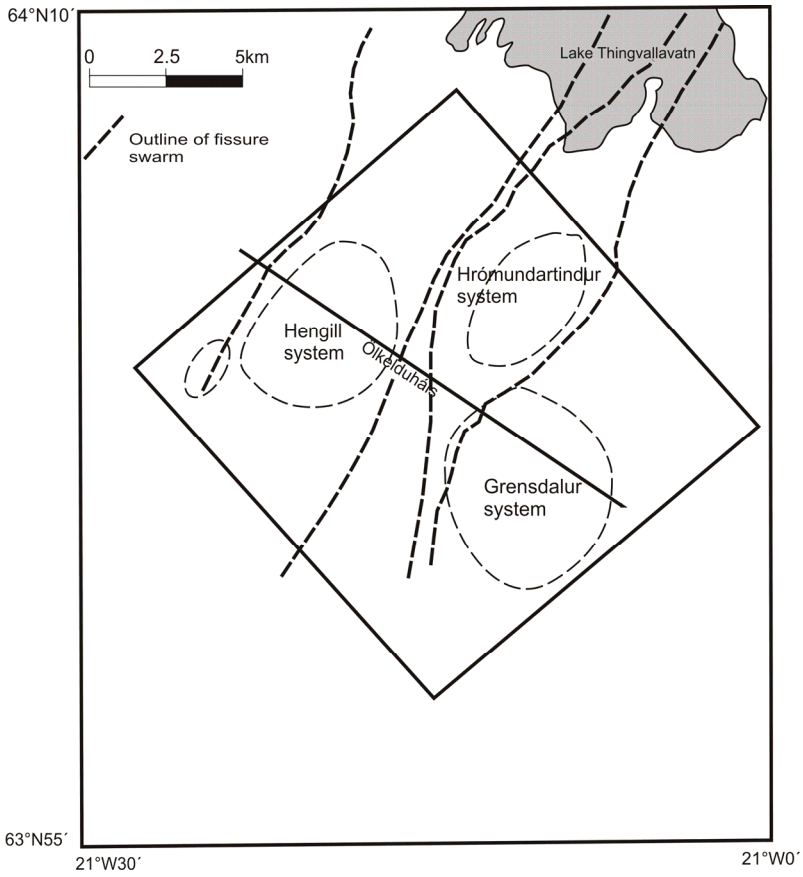

FIGURE 3: Tectonic settings and volcanic systems within the Hengill area (Árnason et al., 1986)

2.2 Alteration of the rocks

Within high-temperature geothermal areas the reaction of the original rocks with hot water or steam results in a complex series of devitrification, recrystallization, solution and deposition reactions which are referred to as hydrothermal rock alteration. The end products of hydrothermal alteration depend on many factors, such as: temperature, pressure, water composition, time of reaction, rate of water and steam flow, and permeability of the rocks, whether permeability is of fissure type or bulk porosity type. In most geothermal areas, hydrothermal alteration zones are observed with increasing depth, temperature, porosity, and changing chemical conditions. In the Icelandic geothermal systems, glass and olivine are the first minerals that alter, at temperatures about 50°C; and at temperatures above 200°C both of them are usually completely altered (Franzson, 1998) (Figure 4).

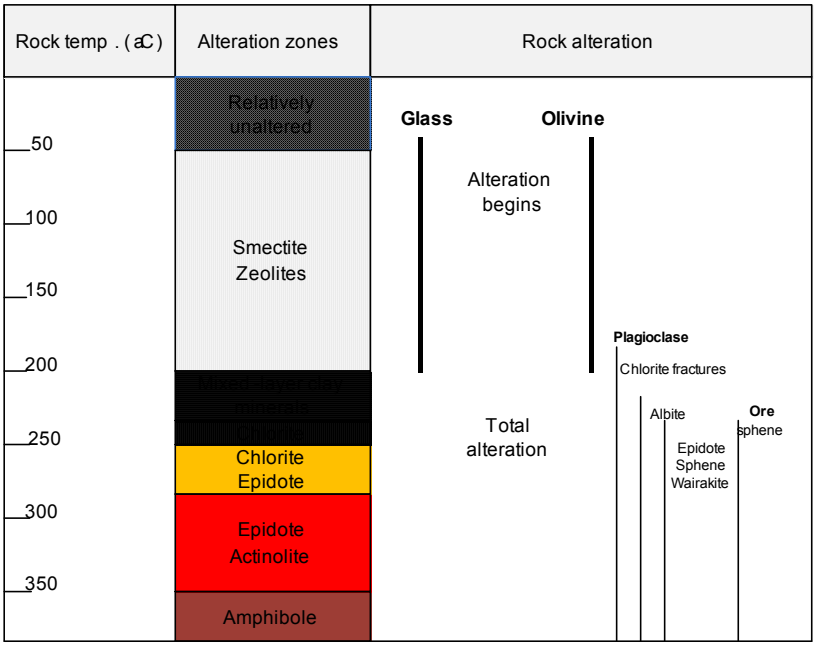

FIGURE 4: Alteration in the Hengill geothermal system (Franzson, 1998)

Rocks in the Hengill geothermal area have been affected by hydrothermal alteration. In Mt. Hengill, acid leaching is usually more or less restricted to steam fields, which are characteristically located on faults. The hyalocalstites in these areas show an extensive alteration of palagonite and clay minerals, mostly smectite. In the oldest rocks north of Hveragerdi, an area about 3 km in diameter shows a regional alteration to pale green colours due to chloritization. Calcite and pyrite are abundant secondary minerals in this zone. The boreholes near Hveragerdi show, according to Sigvaldason (1963), a distinctive secondary mineral zoning.

Well HE-22 is an exploratory well drilled in the Ölkelduháls field, situated on the eastern flank of the Hengill volcanic and geothermal complex. The intercepted rock succession consists of hyaloclastite formations and lava flows of basaltic composition as well as minor intrusive rocks. The formations host a wide variety of secondary hydrothermal assemblages from low- to high-temperature minerals. Four main alteration zones have been identified. These are: the smectite-zeolite zone (<200°C) at <170 m; the mixed-layer clay zone (200-230°C) from 170 to 206 m; the chlorite zone (230-240°C) from 206 to 364 m; and the chlorite-epidote zone (>240°C) from 364 to 740 m. The relationship of time and mineral crystallisation indicates formation from low-temperature alteration at shallower levels to high-temperature alteration in the deeper part of the well (Pendon, 2006).

HE-11 is a 1652 m deep well in the Hellisheidi high-temperature field to the south of Mt. Hengill. The lithology comprises predominantly volcanic rocks of basaltic composition that include lava flows and sub-glacial hyaloclastites formations. Several basaltic intrusions intrude the hyaloclastites. Hydrothermal alteration also indicates four alteration zones in this well: The uppermost part of the well is characterised by no alteration down to 486 m. The first zone is characterised by smectite and zeolites and is situated at 486-700 m with temperatures less than 200°C; the second alteration zone is a mixed-layer clay zone at a depth at 700-756 m with the alteration temperature range 200-230°C. The third is the chlorite zone (756-950 m) with the temperature range 230-250°C; and the fourth the chlorite-epidote zone (>950 m) with temperatures >250°C. The time related mineral deposition sequence shows a geothermal system undergoing a progressive temperature increase over time (Hartanto, 2005).

In Nesjavellir well NJ-20 four alteration zones were found: the smectite-zeolite zone (from top to 360 m); the mixed-layer clay zone (360-820 m); the chlorite-epidote zone at 820-940 m and 1010-1180 m; with the epidote-actinolite zone in between at 940-1010 m (Nouraliee, 2000). In geothermal fields in Iceland, the same zoning sequence is observed; the only difference is the depth at which the alteration occurs (Kristmannsdóttir, 1979).

3. USE OF ISOTOPES AND CHEMISTRY IN GEOTHERMAL INVESTIGATION

Geochemistry, including isotope geochemistry, has greatly contributed to the present understanding of geothermal systems. Ellis and Mahon (1977) suggested that the detection of even small changes in the chemical composition of a geothermal fluid enables a precise assessment of the long term stability of the field. The chemical and isotopic composition of geothermal fluid components provides information on their origin, their recharge area and flow patterns, and may allow an evaluation of subsurface temperatures. In addition, cooling processes of the fluid during the ascent to the surface, due to heat conduction, admixture with cold water, or steam losses, can be studied by means of the changes in the chemical and isotopic composition of the geothermal fluid.

3.1 Natural isotopes

Isotope techniques are a valuable tool in geothermal prospecting as well as for studying the evolution of geothermal fields as a consequence of production. Among the various isotopes, the variations in

stable isotopes of oxygen, hydrogen and carbon provide the most useful information. In this study both hydrogen and oxygen isotopes will be used.

In the discussion of isotopic techniques for geothermal waters, the following terminology is used for geothermal water:

Meteoric water: Water of any age that originated as precipitation, such as rain, snow, polar ice, rivers, lakes and most groundwater, circulates in the uppermost 2-3 km of the earth.
Magmatic water: Water that has equilibrated with magma, regardless of its origin.
Juvenile water: Water from the earth´s mantle core that has never been involved with the hydrosphere.

In earlier times, the origin of water in high-temperature geothermal systems had puzzled geochemists. No geochemical tools were then available to identify it and the most generally accepted theory was that the water was, at least partially, of magmatic and or juvenile origin, i.e. water ascending to the crust through the mantle.

After the development of isotopic methodology, Craig (1963) showed the probable meteoric origin of geothermal waters by measuring the hydrogen and oxygen isotopic composition of water and steam from geothermal fields. He assumed that juvenile water has uniform, albeit an unknown, D/H ratio. He pointed out that at any rate it can certainly be assumed that the isotopic composition of such water is completely independent of the isotopic composition of precipitation on the earth´s surface. No one has been able to prove that juvenile water exists.

An important aspect of geothermal investigation is to determine the recharge to geothermal systems. Craig (1963) established the isotopic characteristics (δ^2H and δ^{18}O) of precipitation in relation to latitude and elevation as well as to continental effects. Samples from higher latitudes and elevation or those collected further inland were progressively lighter (more negative values of δ). δ denotes the relative difference in the ratio of the heavy isotope to the more abundant light isotopes of the sample with respect to a reference standard. This is defined as follows:

$$\delta_{sample} = (R_{sample} - R_{std} / R_{std})\ 1000‰ \quad (1)$$

where the *R´*s are the $^{18}O/^{16}O$ or $^{2}H/H^{1}$ concentration ratios of the sample and a standard (std).

Positive values show the samples to be enriched in the heavy-isotope species with respect to the reference standard; negative values correspond to samples depleted in the heavy isotope species compared to the standard. As the difference between samples and reference standard are usually quite small, it is convenient to express the δ-values in "per mille".

The instrument used to measure isotopes is the *mass spectrometer*. It can detect the tiniest differences in the mass of atoms and molecules (a speck of a difference in mass). A mass spectrometer consists of a tube in which high vacuum is maintained, with an ion source placed at one end of the tube and ion collectors at the other end. Figure 5 shows how a mass spectrometer works. Ions (atoms or molecules without their normal number of electrons) are shot past a strong magnet and their paths are bent by its magnetic field. The smaller the mass of the ion, the more its course is bent, and the greater the mass the less it is deflected from its path. The two isotopes are separated and counted. The illustration in Figure 5

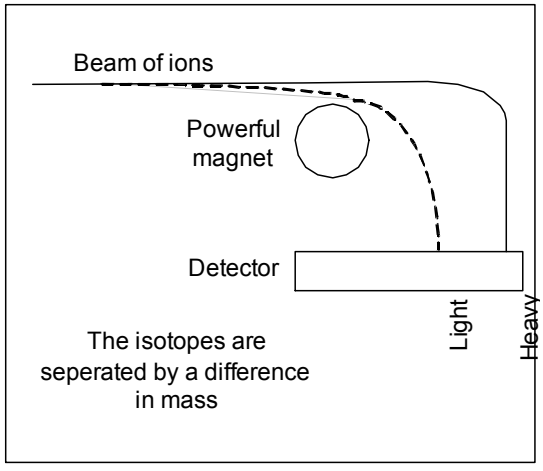

FIGURE 5: The basic layout of a mass spectrometer

explains how the different molecules are separated and counted. A sample of water would have millions of light ions for each heavy ion.

One of the most serious problems in stable isotope studies is the comparison of results obtained by different laboratories. Results are usually reported in δ (‰) with respect to a common international reference standard. Thus, a correct calibration of reference samples is used by different laboratories in routine measurements with respect to international standards, necessary for inter-comparison of results. The standard almost universally adopted as a reference for oxygen and hydrogen stable-isotope variations in natural waters is the VSMOW – Vienna Standard Mean Ocean Water (Gionfantini, 1978).

In any geothermal area, areal variations in the isotopic composition of the discharged fluid (water and/or steam) are generally observed. Rain water infiltrates the permeable outcrops, and springs and wells, fed by this water before any appreciable exchange between water and rocks takes place, will reflect its meteoric origin. In low-temperature geothermal systems the rate of the oxygen isotope exchange reaction between water and minerals is very low. As a consequence, a long contact time is needed to change the water isotopic composition to a detectable extent. Equilibrium will generally not be reached during long residence times in the reservoir. At higher temperatures the $^{18}O/^{16}O$ ratio can change considerably, as a consequence of isotopic exchange with the rocks constituting the geothermal reservoir. For oxygen isotopes, the extent of exchange depends on the relative proportions of oxygen in the water and in the rocks, on the initial ^{18}O contents and on specific water mineral fractionation factors (which are temperature dependent), and on time and extent of surface contact. The exchange process, which is commonly referred to as an oxygen shift, is usually negligible at low temperatures owing to its very slow rates and is greatly accelerated at the high temperature of geothermal fields, with the result that the ^{18}O content of water increases while that of rock decreases (Panichi et al., 1974). As basaltic rocks contain very little hydrogen, there is hardly any hydrogen isotope exchange between rock and water and, therefore, the deuterium value for thermal water still characterizes that of the original fluid.

During the rise of a high-temperature (>100°C) geothermal water, its vapour pressure will at some stage exceed hydrostatic pressure and it will start to boil. These vapour separation processes are accompanied by isotopic fractionation with the heavier isotopes, deuterium and Oxygen-18, portioning into the liquid phase; the separated vapour phase becomes depleted. For deuterium this is true only to about 220°C; at higher temperatures it partitions preferentially into the vapour phase. Because of the rapid rate of isotopic equilibration between water and steam underground liquid-dominated systems were found to correspond effectively to the single step process (Giggenbach, 1988). In this case, the composition of separated vapour, δv and liquid δl, is related to the total discharge composition through the mass balance:

$$\delta d = (1-y)\,\delta l + y dv \tag{2}$$

where y is the fraction of steam formed, which may be obtained from:

$$y = (H_d - H_l)\,/(H_v - H_l) \tag{3}$$

where H_d, H_v and H_l are the enthalpies of total discharge, separated vapour and separated liquid at the separation temperature, respectively.

The world meteoric water line, also known as GMWL (Global Meteoric Water Line), $\delta D = 8(\delta^{18}O)+10$ (Craig, 1961) gives approximate composition of precipitation on earth (Figure 6). The arrow to the right shows the effects of extensive water rock interaction at high temperatures (i.e. oxygen shift). This happens because the water exchanges oxygen with the host rock which has relatively heavy isotopic ratios compared to the water. Hydrogen is less affected by this process because there is so

much more hydrogen in water than in the rocks. In Iceland the $\delta^{18}O$ - δD relationship of the cold groundwater has been defined as (Sveinbjörnsdóttir et al., 1995):

$\delta D = 6.5\ \delta^{18}O - 3.5$ for $\delta^{18}O \geq$ -10.5‰;
$\delta D = 8\ \delta^{18}O + 11$ for lighter precipitation.

The correlation coefficient is 0.97 for both lines.

Árnason (1976) showed how the deuterium values in precipitation in Iceland generally decreased from the coastal areas inland. The highest values were found in the coastal areas: -50‰ on the south coast and -66‰ on the north coast. The lowest values were found in north central Iceland -106‰ in the northern part of the Vatnajökull ice cap (Figure 1). By his measurements he showed that all ground waters in Iceland are meteoric. However, the deuterium content of cold and hot spring water is often different from the deuterium content of the local precipitation. By comparing the results obtained and Árnason's deuterium map of present precipitation in Iceland (Árnason, 1976) it is often possible to deduce where the spring water might have fallen as precipitation and therefore determine its flow path from recharge to discharge areas.

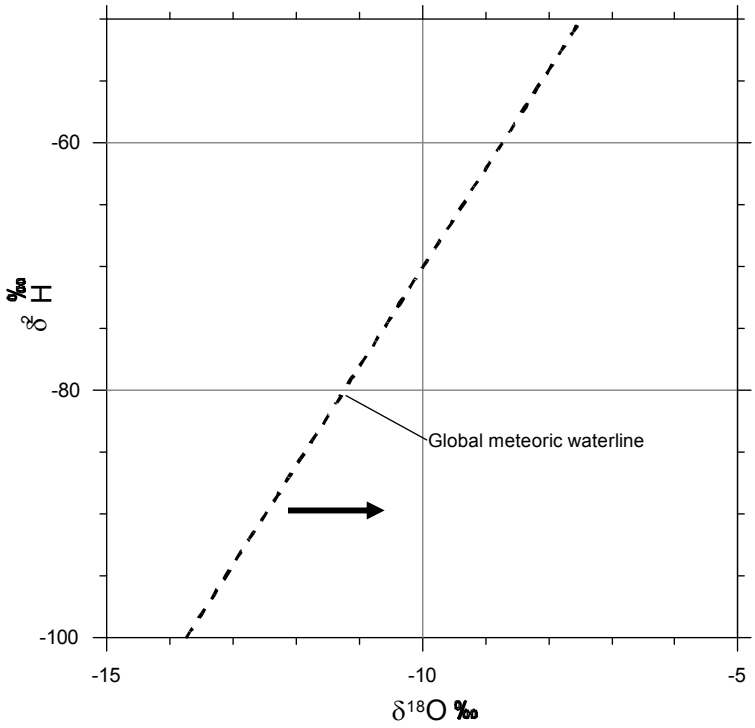

FIGURE 6: The global meteoric waterline

3.2 Cl-SO4-HCO_3 diagram

Giggenbach (1991) proposed a SO_4-Cl-HCO_3 ternary diagram for the initial classification of geothermal solutions to identify whether the geothermometers are applicable for the given water sample, as most solute geothermometers work only for neutral waters. According to Giggenbach (1991), solute geothermometers can only be applied to what is referred to as "mature waters", characterized by high Cl and low SO_4. This diagram is also helpful in providing an initial indication of mixing relationships or geographic groupings.

The position of a data point in such a triangular diagram is obtained by first obtaining the sum S of the concentrations of all three constituents involved. In the present case:

$$S = C_{Cl} + C_{SO4} + C_{CHO3} \tag{4}$$

The next step consists of the evaluation of % Cl, $\%SO_4$ and $\%HCO_3$ according to the following:

$$\%Cl = 100\ C_{CL}/S; \quad \%SO_4 = 100\ C_{SO4}/S; \quad \%HCO_3 = 100\ C_{HCO3}/S \tag{5}$$

The degree of separation between data points for high chloride and bicarbonate waters gives an idea of the relative degree of interaction of CO_2 charged fluids at lower temperatures, and the HCO_3 contents increasing with time and distance travelled.

3.3 Geothermometry

Temperature sensitive equilibria between minerals, geothermal solutions and, in some cases, a vapour phase can affect the chemical composition of a geothermal fluid, providing the basis for chemical geothermometry. Chemical geothermometers are normally applied to thermal springs, steam vents, and geothermal wells for inferring reservoir temperatures in geothermal exploration and exploitation. The most widely used geothermometers are based on silica concentrations, cation ratios (mainly Na/K). Selected geothermometers of these types are described below.

3.3.1 Silica geothermometers

Temperature-sensitive quartz solubility controls the silica concentration in geothermal fluids in high-temperature geothermal systems. Considerable efforts have been made to measure the quartz solubility and interpret the silica concentrations in thermal springs and geothermal wells. Morey et al. (1962) and Fournier and Rowe (1962) plotted the logarithm of the concentration of dissolved silica versus the reciprocal temperature for quartz and various phases of silica, respectively. They discovered that the data fell along a straight line over the temperature range 20-250°C. Fournier presented the first geothermometer in equation form (Fournier, 1977) and later with his co-workers (Fournier and Potter, 1982) derived a polynomial equation for the quartz geothermometer that estimates temperature up to 330°C. The Fournier and Potter (1982) quartz geothermometer is based on several assumptions, including that the fluid is in equilibrium with quartz in the reservoir, the vapour pressure of pure water fixes the pore fluid pressure in the reservoir, there is no mixing of hot and cold water during upflow, and lastly there is either conductive cooling of the ascending water or adiabatic cooling with steam separation at 100°C (Fournier, 1991). The quartz geothermometer of Fournier and Potter (1982) has been widely used. Later, various silica geothermometers have been developed to assess reservoir temperatures from the silica content of natural water in equilibrium with either quartz or chalcedony. Temperatures predicted by these geothermometers are referred to as quartz- and chalcedony temperatures, respectively (Arnórsson, 2000). Generally speaking, the quartz geothermometer is applied in high-temperature reservoirs, and the chalcedony geothermometer in low-temperature reservoirs. The SiO_2 geothermometer is normally based on a polynomial function describing experimentally determined silica solubility as a function of temperature (Fournier and Potter, 1982). The basic principle reaction describing silica solubility is: where SiO_2-solid is either quartz or chalcedony and SiO_2-aq refers to aqueous silica.

At pH levels below ~9, nearly all dissolved silica is present in solution as undissociated silicic acid, H_4SiO_2. At higher pH levels, the silicic acid dissociates to form H_3SiO_4-, thus effectively increasing the solubility of silica in water in equilibrium with quartz. Therefore, very high pH levels can lead to over estimation of the reservoir temperature if aqueous speciation of silica is not considered. Several geothermometers have been developed as more experimental data has become available (e.g. Gunnarsson and Arnórsson, 2000). Verma and Santayo (1997) have recently developed a new silica geothermometer based on statistical treatment of earlier experimental data. Their new geothermometer is proposed through detecting an outlier and rejecting one sample from the data set of Fournier and Potter (1982). The quartz geothermometer was tested experimentally over the temperature range from 100 to 500°C and pressure of 1000 bars, performed well up to 400°C without any effect of fluid composition (Pope et al., 1987). However, Verma (2000) criticized the use of the quartz geothermometer, especially its discrepancy at high temperatures arising from the incoherence between the theoretical and experimental solubility data. The silica geothermometers equations used to calculate the temperature of a reservoir are as follows:

Quartz, no steam loss, temperatures between 25 and 250°C (Fournier, 1977):

$$t(°C) = \frac{1309}{5.19 - logS} - 273.15 \quad (6)$$

Quartz, maximum steam loss at 100°C, temperatures between 25 and 250°C (Fournier 1977):

$$T(°C) = \frac{1522}{5.75 - \text{Log S}} - 273.15 \quad (7)$$

Quartz, 25-900°C (Fournier and Potter, 1982):

$$T(°C) = -42.2 + 0.28831\ S - 3.6686 \times 10^{-4}\ S^2 + 3.1665 \times 10^{-7}\ S^3 + 77.034 \log S \quad (8)$$

Quartz, after adiabatic boiling to 100°C (Fournier and Potter, 1982):

$$T(°C) = -53.5 + 0.11236\ S - 0.5559 \times 10^{-4}\ S^2 + 0.1772 \times 10^{-7}\ S^3 + 88.390 \log S \quad (9)$$

Quartz, 0-350°C (Arnórsson, 2000):

$$T(°C) = -55.3 + 0.36590\ S - 5.3954 \times 10^{-4}\ S^2 + 5.5132 \times 10^{-7}\ S^3 + 74.360 \log S \quad (10)$$

Quartz, after adiabatic boiling to 100°C (Arnórsson, 2000):

$$T(°C) = -66.9 + 0.13780\ S - 4.9727 \times 10^{-5}\ S^2 + 1.0468 \times 10^{-8}\ S^3 + 87.841 \log S \quad (11)$$

Quartz, for the temperature range 20-210°C (Verma and Santayo, 1997):

$$T(°C) = -44.119 + 0.24469\ S - 1.7414 \times 10^{-4}\ S^2 + 79.305 \log S \quad (12)$$

Quartz, for the temperature range 210-310°C (Verma and Santayo, 1997):

$$T(°C) = 140.82 + 0.23517\ S \quad (13)$$

Chalcedony, 0-250°C (Fournier, 1977):

$$T(°C) = \frac{1032}{4.69 - Log\ S} - 273.15 \quad (14)$$

Chalcedony (Arnórsson et al., 1983):

$$T(°C) = \frac{1112}{4.91 - Log\ S} - 273.1 \quad (15)$$

where S refers to the concentration of SiO_2 in ppm and T is the temperature.

3.3.2 Cation geothermometers

Cation geothermometers are commonly used to estimate reservoir temperatures. Of the cation geothermometers, the Na-K geothermometer is most widely used. The Na-K ratio was initially used to identify the upflow zone of a geothermal system, where the lowest values are observed at the centre of the upflow zone (Ellis and Wilson, 1960). Since then, this method has evolved to an increasingly more precise calibration of the temperature dependence of the Na/K ratio, resulting in the calibration of the Na/K geothermometer. The partitioning of sodium and potassium between aluminosilicates and aqueous solutions is strongly temperature dependent. This is generally interpreted as a result of equilibrium between Na- and K-feldspars and the aqueous solution, described by the reaction:

$$K + Na\text{-}feldspar = K\text{-}feldspar + Na+$$

The Na-K geothermometer generally gives consistent results for near neutral pH of geothermal waters that have low calcium content, ($\sqrt{Ca}/Na$) < 1. The Na/K geothermometers are generally in agreement with quartz geothermometers but sometimes they yield rather high results. Solute geothermometers, including those based upon silica solubility and Na/K and K^2/Mg ratios (Giggenbach, 1988) are ideally applied to chloride springs but are considered less reliable when applied to low-chloride springs.

Based on this principle, various Na/K cation geothermometers have been developed and applied to geothermal exploration (e.g. Fournier and Truesdell, 1973). Nieva and Nieva (1987) presented a geothermometer based on cation exchange and argued that the geothermometer is able to predict the reservoir temperature, based on the composition of relatively dilute hot-spring waters. Recently, a new Na/K geothermometer was developed purely on an empirical basis and calibrated from field data (Can, 2002).

The *cation geothermometers* considered in this study are listed below. *Na*, *K*, and *Ca* refer to the concentrations of these cations in solution in ppm:

Truesdell (1976) for 100-275°C:

$$T(°C) = \frac{856}{0.857+\log\left(\frac{Na}{K}\right)} - 273\,.\,15 \tag{16}$$

Tonani (1980):

$$T(°C) = \frac{883}{0.78+\log\frac{Na}{K}} - 273.15 \tag{17}$$

Arnórsson et al. (1983) for 25-250°C :

$$T(°C) = \frac{933}{0.993+\log\frac{Na}{K}} - 273.15 \tag{18}$$

Arnórsson et al. (1983) for 250-350°C:

$$T(°C) = \frac{1319}{1.699+\log\frac{Na}{K}} - 273.15 \tag{19}$$

Fournier (1979):

$$T(°C) = \frac{1217}{1.483+\log\frac{Na}{K}} - 273.15 \tag{20}$$

Nivea and Nieva (1987):

$$T(°C) = \frac{1178}{1.47+\log\frac{Na}{K}} - 273.15 \tag{21}$$

Giggenbach et al. (1983):

$$T(°C) = \frac{1390}{1.75+\log\frac{Na}{K}} - 273.15 \tag{22}$$

Can (2002):

$$T(°C) = \frac{1052}{1+e^{1.714\left(\frac{Na}{K}\right)+0.252}} + 76 \quad (23)$$

Fournier and Truesdell (1973):

$$T(°C) = \frac{1647}{\log\frac{Na}{K}+\beta\left(\log\left(\frac{\sqrt{Ca}}{Na}\right)+2.06\right)+2.47} \quad (24)$$

where $\beta = 4/3$ for T<100°C; and $\beta = 1/3$ for T > 100°C.

The Na, K, Ca, and Mg total contents, as well as the Na^2/Mg and Na^2/Ca ratios, are mainly controlled by ionic salinity and are, therefore, hardly suitable for geoindicators (Chiodini et al., 1991). The experimental work of Pope et al. (1987) showed that the Na-K-Ca geothermometer performed well in 0.1 *M* NaCl solution, but did not work well for experiments using 0.01 M $NaHCO_3$. They concluded that the Na-K-Ca ratio is controlled by alteration reactions, i.e. by base exchange involving clays and mica rather than feldspar equilibria.

3.4 The Na-K-Mg ternary diagram

The Na-K-Mg ternary diagram (Giggenbach,1988) can be used to classify waters into full equilibrium, partial equilibrium and immature waters (dissolution of rock with little or no chemical equilibrium). The full equilibrium curve is for reservoir water composition corrected for loss of steam owing to decompressional boiling. Uncorrected boiled waters will generally plot slightly above the full equilibrium line. The diagram can be used to better clarify the origin of the waters, and then determine whether the fluid has equilibrated with hydrothermal minerals and to predict the equilibrium temperatures, $T_{Na\text{-}K}$ and $T_{K\text{-}Mg}$. The diagram is based on the temperature dependence of the three reactions:

$$K\text{-}feldspar + Na^+ = Na\text{-}feldspar + K^+$$

$$2\ albite + 0.8\ K\text{-}feldspar + 1.6\ H_2O + Mg^{2+} = 0.8\ mica + 0.2\ chlorite + 5.4\ silica + 2\ Na^+$$

$$2.8\ K\text{-}feldspar + 1.6\ H_2O + Mg^{2+} = 0.8\ mica + 0.2\ chlorite - 5.4\ silica + 2\ K^{2+}$$

A large number of samples can be plotted simultaneously on this diagram, and mixing trends and grouping predicted. The sum is calculated as:

$$S = {}^{C_{Na}}/_{1000} + {}^{C_K}/_{100} + \sqrt{C_{Mg}}$$

Then the %Na", %K" and %Mg", can be calculated as:

$$\%\text{Na} = \frac{C_{Na}}{10S}; \qquad \%\text{K} = \frac{C_K}{S} \qquad \text{and} \qquad \%\text{Mg} = \frac{\sqrt{C_{Mg}}}{S}$$

where *C* is in mg/l.

The geothermometer equations used for evaluation of the temperatures in the Na-K-Mg system are Equation 22 for Giggenbach's (1988) data, or Equations 18 and 19 for Arnórsson et al.'s (1983) data with

$$T_{K\text{-}Mg}(°C) = 4410 / (14.0 - \log(K^2/Mg) - 273.15 \quad (25)$$

where *Na, K* and *Mg* refer to the concentrations of the respective cations.

Evaluation of analytical data for *Na, K* and *Mg* using the ternary diagram allows a clear distinction to be made between waters suitable or unsuitable for the application of ionic solute geothermometers.

3.5 Mineral saturation

Evaluation of chemical equilibria between minerals and aqueous solutions in natural systems requires determination of the activities of aqueous species and knowledge of the solubilities of the minerals present in the bedrock. Assumption of specific mineral-solution equilibria is necessary to use in applying geochemistry to obtain an understanding of various physical features of a geothermal system. In this study, the WATCH chemical speciation program (Arnórsson et al., 1982), version 2.1A (Bjarnason, 1994), was used to calculate aquifer water compositions from the analytical data for some water and steam samples collected at the wellhead. The saturation index of several minerals is computed as a function of temperature and if the saturation indices of the minerals converge to zero (saturation) at a specific temperature, that temperature is taken to represent the reservoir temperature. However, it is to be noted that care should be taken in interpreting the results of multi-mineral/solute equilibria, as the results depend on both the thermodynamic data base used for mineral solubilities and the activities of end-member minerals in solid solutions (Tole et al., 1993). Using the results of the aqueous speciation calculations, the saturation indices (SI) of minerals in aqueous solutions at different temperatures were computed as:

$$SI = \log Q - \log \mathrm{K} = \log Q/K$$

where Q is the calculated ion activity product (IAP) and K is the equilibrium constant.

The *SI* value for each mineral is a measure of the saturation state of the water phase with respect to the mineral phase. Values of *SI* greater than, equal to, and less than zero represent supersaturation, equilibrium and undersaturation, respectively, for the mineral phase with respect to the aqueous solution. Equilibrium constants for mineral dissolution often vary strongly with temperature. Therefore, if the *SI*s with respect to several minerals converge to zero at a particular temperature, that temperature is taken to be the reservoir temperature. For the WATCH calculations of aquifer water compositions, it was assumed that the cause of the excess enthalpy was phase segregation in the producing aquifer (Arnórsson, 2000; Gudmundsson and Arnórsson, 2005).

4. SAMPLING AND ANALYTICAL METHODS

Sample collection, chemical analysis and data interpretation are the three main steps involved in geochemical studies of geothermal fluids. A brief description of the sampling techniques, sample treatment and analytical techniques adopted here is given in this section. For detailed sampling and analytical techniques, see Paces (1991), Arnórsson (1991), Ármannsson and Ólafsson (2006) and Pang and Ármannsson (2006).

4.1 Sampling

The types of samples used in this study are water samples from hot water wells and water samples from wet-steam water wells. The collection of representative gas samples from a discharging well involves the collection of dry gas (non-condensable gases), condensate, steam (in NaOH solution) and hot water. It should be conducted with the aid of a Webre separator and a cooling device. Great care should be taken to separate steam completely from liquid.

Sample treatment is specific for particular analytical methods. Usually, the water samples were collected in several fractions:

Ru samples are raw and untreated for CO_2 and H_2S analysis;
Rd samples are raw and diluted on site with de-ionised water to bring SiO_2 <100 ppm for analysis;
Fu samples are filtered and untreated for anion analysis;
Fp samples are filtered and precipitated for SO_4 analysis;
Fa samples are filtered for cation analysis.

Samples for isotope analysis were collected in 60 ml bottles; they were also raw and untreated.

TABLE 1: Analytical methods for geothermal fluids

Composition	Sample fraction	Methods of analysis
CO_2	Ru	Alkalinity-titration
H_2S	Ru	Titration
SiO_2	Rd	Spectrophotometry
Na	Fa	Atomic absorption spectrometry
K	Fa	Atomic absorption spectrometry
Ca	Fa	Atomic absorption spectrometry
F	Ru	Ion selective electrode
Cl	Ru	Ion chromatography
SO_4	Fp	Ion chromatography
Al	Fa	Atomic absorption spectrometry
Fe	Fa	Atomic absorption spectrometry
$\delta^{18}O$, δD	Ru	Mass spectrometry
pH	Ru	Ion selective electrode

4.2 Analytical methods

The analytical methods used to obtain the data for the report are presented in Table 1. All chemical data are reported in the relevant sections.

5. CHEMICAL AND ISOTOPIC CHARACTERISTICS OF THE THERMAL FLUIDS

The results presented here are based on several analyses of fluid samples and on the results of previous work. Table 2 shows the data from 2000-2007 from the Nesjavellir geothermal field, while Table 3 shows similar data from the Hellisheidi geothermal field. The fluid samples, collected between July-August 2007, were also analysed for stable isotopes at the University of Iceland using the "Delta-V-Advantage thermo" mass spectrometer. The results are shown in Table 4. Chemical data on the thermal fluids from Hveragerdi and Nesjavellir collected and analysed in the years 1980-1990 is from the ÍSOR database. Chemical and isotopic data have been compiled and contoured on maps in order to study the chemical and thermodynamic properties of the field.

5.1 The Nesjavellir geothermal field

5.1.1 Stable isotopes before production started

In the years 1985-1989 stable isotope measurements were performed on hydrothermal fluids from 15 wells in the Nesjavellir area (Sveinbjörnsdóttir, 1989). The measurements were carried out using the Finnegan MAT 251 mass spectrometer at the Science Institute, University of Iceland. The results are shown in Table 5. Production from the Nesjavellir field had not started at that time. Figure 7 shows a graph for δ^2H vs. $\delta^{18}O$ for the thermal fluid at Nesjavellir using only data from the 1980s. The figure demonstrates a considerably larger oxygen shift for wells located east of the youngest eruption fissure with a mean $\delta^{18}O$ value of -6.5‰ than for wells situated west of the fissure where the mean $\delta^{18}O$ value is -8.0‰. No difference was observed in the δ^2H values in wells east and west of the fissure with the mean value of -75‰, indicating the same fluid to be present within the whole production area. This value for the deep circulating fluid in the Nesjavellir area is considerably lighter than that of the local precipitation, estimated of about -60‰ (Sveinbjörnsdóttir and Johnsen, 1992), indicating a

TABLE 2: Nesjavellir wells, analys es of fluid samples (mg/kg) in 2000-2007

Well no.	Date	Sample no.	Ps (bar)	Av. Ps (bar)	Ts (aC)	Ho	pH /aC	CO_2	H_2S	SiO_2	Na	K	Ca	Mg	SO_4	Cl	F
NG-5	16.3.2000	5048	15.8	15.8		1900.0	8.59 24.0	56.7	85.3	694.8	152.2	27.8	0.26	0.01	18.9	114.7	1.0
NG-6	4.10.2000	5095	16.2	16.0	195.2	2235.0	8.36 22.0		66.9	773.0	143.3	27.5	0.18	0.00		198.0	
NG-6	27.8.2004	5092	15.8			2193.0	8.75 21.8	17.8	51.1	636.9	154.5	29.3	0.28	0.01		167.5	0.7
NG-7	25.2.2000	5044	15.5	15.0		1050.0	9.18 20.2	56.2	96.4	662.0	165.2	27.4	0.38	0.00	44.1	113.0	1.3
NG-7	7.6.2006	5085	13.7			1343.0	9.02 23.6	70.9	91.7	672.9	173.2	30.6	0.56	0.02	15.6	113.7	
NG-10	25.2.2000	5045	15.5	15.5		1140.0	9.36 21.3	32.0	75.3	715.0	163.3	29.1	0.35	0.01	21	121.6	1.7
NJ-11	16.3.2000	5049	15.8	15.5		1900.0	8.76 24.1	20.8	121.0	764.7	133.4	23.8	0.39	0.00	54.2	75.5	1.1
NJ-11	28.9.2000	5094	15.5		192.8	2247.0	9.08 22.0	14.6	111.0	804.0	145.5	24.6	0.41	0.02		67.5	
NJ-13	4.10.2004	5093	16.6	16.6	196.6	1936.0	8.71 22.1	16.1	62.2	700.6	141.2	28.1	0.14	0.02		152.6	0.9
NJ-14	4.2.2000	5018	15.5	15.0		1400.0	9.27 23.0	26.0	43.6	716.0	162.8	30.2	0.27	0.00	22.7	206.7	1.3
NJ-14	22.7.2003	5117	14.0		190.7	1195.0	9.3 22.7	21.9	32.5	707.1	163.7	30.2	0.3	0.00	3	232.1	
NJ-16	16.3.2000	5050	16.2	14.1		1650.0	8.86 24.2	27.4	138.0	720.0	148.2	26.7	0.35	0.00	88.5	115.0	1.2
NJ-16	9.11.2000	5097	4.3		153.4	1520.0		17.6	112.0	791.0	154.7	27.2	0.34	0.01		94.0	
NJ-16	12.6.2006	5086	14.1			1784.0	8.82 23.1	44.5	124.0	697.6	160.3	29	0.5	0.02	33.7	88.6	
NJ-19	4.5.2000	5070	16.2			2000.0	8.05 22.0	11.0	67.6	815.3	119.1	25.1	0.09	0.00	58.8	116.3	1.1
NJ-19	8.2.2002	5034		17.4	199.8	1993.0	8.41 21.4	0.0	74.3	908.0	131.2	26.9	0.09	0.00	25.6	144.4	1.3
NJ-19	4.10.2004	5094	17.4		187.8	73.0	8.61 22.2	19.1	62.7	692.4	142.4	28	0.09	0.00		159.4	1.0
NJ-19	14.8.2006	5094	13.6			1954.0	8.43 22.6	13.7	65.9	825.8	144.7	32	0.3	0.03	6.3	152.7	
NJ-20	4.2.2000	5017	9.0	9.0		1386.0	9.02 23.1	32.3	54.6	725.0	173	31.7	0.42	0.00	27.3	173.5	0.1
NJ-21	27.3.2001	5060	14.0			2265.0	9.19 22.7	109.5	108.8	878.7	195.4	33.4	0.81	0.02	29	166.4	0.7
NJ-21	2.5.2001	5068	3.7	14.0	151.1	2627.0	9.47 22.0	217.6	11.3	1069.0	207.5	37.9	0.87	0.05	52.2	221.4	1.0
NJ-21	7.2.2002	5033			151.1	2348.0	6.18 22.0	402.8	166.4	759.0	160.9	28.1	0.36	0.01	35.9	113.2	1.4
NJ-21	27.6.2006	5090	14.0			2528.0	8.67 22.7	77.6	99.8	747.3	151.7	29.5	0.48	0.02	11.4	114.4	
NJ-22	27.3.2001	5058	14.0			1781.0	8.61 21.5	24.1	86.7	771.1	139.9	28.8	0.74	0.02	18.8	203.2	0.7
NJ-22	2.5.2001	5067	13.2	14.0	194.3	1967.0	8.71 22.0	76.5	8.8	771.9	133.4	28.4	0.26	0.01	12.5	200.7	0.7
NJ-22	7.2.2002	5032			194.8	2102.0	7.87 22.4	42.2	47.9	875.0	138.7	29.4	0.23	0.07	25.1	167.4	1.2
NJ-22	19.4.2002	5067			200	1881.0	8.85 24.3	16.9	39.4	770.0	138.5	27.9	0.16	0.01	15.1	163.2	1.2
NJ-22	29.6.2006	5091	14.2			1646.0	8.98 22.8	14.6	48.0	852.2	158.2	35.3	0.18	0.02	6.6	170.4	
NJ-23	17.3.2004	5070	6.0	6.0	163.9		7.1 22.7	106.4	255.0	763.4	159	30.6	0.62	0.09		98.3	1.4

TABLE 3: Hellisheidi wells, analyses of fluid samples (mg/kg) in 2000-2007

Well no.	Date	Sample no.	Ps (bar)	Av. Ps (bar)	Ts (aC)	Ho	pH /aC		CO_2	H_2S	SiO_2	Na	K	Ca	Mg	SO_4	Cl	F
HE-3	16.4.2002	5062	4.3		153.5	1199	9.14	24	18.3	14.1	736.3	218.6	32.3	4.67	0		289.8	
HE-3	14.6.2002	5086	5.2	5	157.8	1330	9.32	24.6	16.4	19.3	599.4	237.7	35.1	1.81	0	44.6	316.5	0.93
HE-3	10.9.2002	5092	5.5		159.6	1396	9.37	22.6	15.2	19.6	658.4	240.1	39.6	0.99	0	22.5	333	0.93
HE-4	16.4.2002	5063	6		163.5	1234	9.46	24.3	19.4	30.5	759.2	175.9	24	1.09	0		244.3	
HE-4	14.6.2002	5087	7	7.5	168.9	1226	9.58	24.9	14.6	31.4	595.8	194.7	26.3	0.77	0	37.8	228.1	0.9
HE-4	10.9.2002	5093	7.5		171.5	1358	9.49	22.7	18.4	35.6	609.4	188.1	27.1	0.6	0	19.2	206.3	0.9
HE-4	1.4.2003	5078	8.7		172	1288	9.44	23.2	13.9	39.6	648.3	187.9	25.7	0.57	0	24.3	257.1	1
HE-5	31.10.2002	5107	6.3		161.2	1017	9.6	21.7	83.7	18.7	561	185.8	26.8	0.61	0	39.1	115	2.01
HE-5	26.11.2002	5108	5.9		163.5	1127	9.56	21.4	77.3	26.7	582	150.1	24.5	0.79	0	22.6	125.9	2.12
HE-5	28.3.2007	5044	8.4	8.4		1194					695.9	1717.9	30	0.36	0	20.2	78.3	
HE-6	11.3.2003	5064	5		158.8	1318	9.29	24				181.7	26.2	1.38	0	60.4	167.8	1.09
HE-6	19.5.2003	5101	7.2	7.2	164.9	1354	9.38	20.7	85.6	32.4	587	175.2	25.6	0.58	0	27.4	200.4	0.97
HE-6	15.7.2003	5106	6.8		165.3	1397	9.28	22.9	51.7	38.6	625.2	171.3	26.5	0.6	0.01	23.2	193.9	
HE-6	12.4.2007	5047	11			1522					806.6	180.1	29.2	0.28	0.01	24.6	119.3	
HE-7	18.12.2002	5109	10.4		177.9	1414	9.6	21.8	0	72.7	629	182	28.5	0.75	0.01	20.6	172.5	0.97
HE-7	11.3.2003	5065	12.5		187.1	1429	9.11	24.1				196.6	21.1	0.48	0	25.2	216.4	1.06
HE-7	19.5.2003	5102	11.5		187.6	1459	9.19	21.3	36.8	56.3	540	189.6	28.9	0.46	0.01	22.3	298.9	1.15
HE-7	15.7.2003	5105	10.5	10	182.5	1239	9.22	22.9	32.8	56	685.3	194.9	31	0.4	0.09		203.9	
HE-7	30.8.2006	5097	6.5			1255				45.6	748.3	203.1	35.7	0.48	0.02	9.5	227.9	
HE-7	26.4.2007	5061	10.1		181.9	1423					712.2	215.8	35.8	0.37	0	95	209.2	
HE-7	17.7.2007	5117	9.3		180.5	1523					728	217.3	36.7	0.36	0.01	10.3	219.8	
HE-8	23.6.2004	5072	2.4	2.4		1213	9.54	22.7	108.3	15.7	649.6	161.8	25.7	2.7	0.1		110.5	1.28
HE-9	17.11.2003	5125	7.2		166.9	2633	8.74	22.2			793.6	175.8	30	1.08	0.01		202.5	
HE-9	18.4.2007	5050	9	9		2757					101.2	87.9	13	0.32	0.01	32.5	56.8	
HE-11	21.10.2004	5100	14.7		191.8	1295	8.66	22	41.2	48.6	728.6	175	31.4	0.55	0.01		186.6	0.69
HE-11	6.12.2006	5133	9.8	11.56	180.1	1836			46.7	59	786.2	179.1	35.2	0.41	0	16.3	173.1	
HE-11	12.4.2007	5048	11.2			1839					715.5	187.8	36.2	0.27	0	49.2	179.5	
HE-12	9.3.2005	5056	11.8	11.8	189.5	1292	9.24	21.8	28	56.1	686.2	176.6	32.9	0.61	0.01		267.3	0.93
HE-13	12.5.2005	5078	5	5		965	9.67	23.2	32.4	33.2	603.4	151	23.6	1.45	0.01		125.5	
HE-15	12.5.2005	5077	8.8	8.8		1174	9.35	22.8	20.7	21.5	640.5	186.1	31.7	0.62	0.01		191.7	
HE-15	15.6.2005	5081	8.8			1241	9.39	24.6	17.2	47.8	651.1	189.3	32.3	0.64	0.01		195.9	
HE-16	9.5.2006	5080	4.2	4.2		1124	9.32	24.4	33.6	45	622.2	201.7	31.9	1.91	0.01	23.6	193.5	
HE-17	15.12.2005	5107	12			1326	9.1	23.3	29	42.6	819.2	182.9	36.2	0.39	0.01		199.8	
HE-17	7.2.2006	5058	10.8			1579	8.88	23		45.9	796.8	176.8	37.8	0.33	0.05		205.5	
HE-17	7.12.2006	5134	11.3	12	187.8	2533	7.95	22	39.5	72	797.5	164.2	32.9	0.69	0	15.8	170.6	
HE-17	3.7.2007	5101	12.5		187.3	2319					848.7	195.9	38		0.01	8.3	203.8	
HE-18	19.4.2006	5077	7.8	21		1236	9.55	22.7	35.6	37	737.7	189.4	33.6	1.37	0.1	9.7	238	
HE-18	18.4.2007	5049	21			1433					119.1	190.5	32.3	0.37	0.01	10.6	157.6	
HE-19	29.3.2007	5045	8.6			1584					642.3	219.4	33.7	0.57	0	10.5	207.8	
HE-19	17.7.2007	5116	8.8	8.8	178.7	1560					640.6	217.1	33.6	0.56	0.01	12.4	208.8	
HE-20	30.5.2006	5083	5	5		1059	8.53	23.5	102.8	44.1	550.3	235.8	32.7	5.29	0.02	37.1	228.7	
HE-20	29.8.2006	5095	4.7	5		1053	8.43	23.7	99.5	44.9	579.1	236.2	32.7	3.38	0.03	50.8	230.2	
HE-20	30.10.2006	5103	8			1069	8.82	23.3	103	52.3	570	232.1	32.5	3.14	0.02	41.5	223.8	
HE-21	30.5.2006	5084	6	6		1885	8	23.8	39.3	8.3	975.8	262.5	59.3	0.67	0.01	5.2	400.2	
HE-21	30.8.2006	5096	5.1			1815	7.87	23.7	34	6.6	1035.5	276.5	65.4	0.6	0.02	6.5	438.5	
HE-22	1.12.2006	5132	3.2	3.2	140	902	9.23	23.2	24.1	47.4	442	221.4	24.7	3.16	0	73.1	217	
HE-23	19.6.2007	5083	2.8	2.8		1279					508.6		171.7	0.93		37.7	111.4	
HE-24	19.6.2007	5084	8	8	171.1	1918					600.1	171.7	25.6	1.22	0.01	46.2	119	
HE-25	20.6.2007	5085	3.9	3.9	142.7	1310					652.5	202.1	28.9	1.1	0.01	47.3	144.6	
HE-27	26.6.2007	5088	5	5	154.9	1752					598.4	227	29.4	5.7	0.01	95	202.8	

faraway origin for the thermal water. The difference in $\delta^{18}O$ can be explained if the geothermal activity within the area west of the fissure is considerably older than the activity east of it (Sveinbjörnsdóttir, 1989).

Figure 8 shows the spatial distribution of $\delta^{18}O$ in Nesjavellir in the 1980s before production from the field started. The highest values are observed along an axis, trending NE-SW, through the field, with the highest values $\delta^{18}O$ -5.9 ‰ and -6.5 ‰. Low values are observed in the north-western part of the field.

TABLE 4: Hellisheidi wells, isotopic analyses of samples from 2007

Easting	Northing	Sample no.	Well no.	$\delta^{18}O$ (l)	$\delta^{2}H$ (l)	$\delta^{18}O$ (s)	$\delta^{2}H$ (s)	Enthalpy, Ho (kJ/kg)	Ho (l) (kJ/kg)	Ho (s) (kJ/kg)	$\delta^{18}O$	$\delta^{2}H$	Ps (bar)	Steam ratio	Cl (mg/kg)
-21.3179	64.0561	5088	HE-27	-5.53	-59.36	-8.88	-69.34	1752.0	623.224	2744.0	-7.313	-64.672	4.50	0.532	190.25
-21.3567	64.0375	5101	HE-17	-4.89	-59.32	-7.25	-62.97	2319.0	782.979	2781.0	-6.704	-62.126	11.10	0.769	212.96
-21.3740	64.0296	5116	HE-19	-5.67	-63.64	-8.44	-68.66	1560.0	727.736	2769.8	-6.799	-65.686	8.30	0.408	198.26
-21.3581	64.0333	5117	HE-07	-5.61	-63.33	-8.16	-67.52	1523.0	746.845	2773.9	-6.586	-64.934	9.20	0.383	239.10
-21.3168	64.0432	5129	HE-11	-5.63	-62.62	-8.04	-65.49	2047.0	789.988	2782.3	-7.151	-64.431	11.50	0.631	179.50
-21.3381	64.0574	5130	HE-23	-5.9	-59.97	-9.91	-74.00	1279.0	551.462	2721.7	-7.244	-64.673	2.80	0.335	
-21.3469	64.0496	5131	HE-25	-5.97	-61.67	-9.27	-72.24	1310.0	604.723	2738.1	-7.061	-65.164	4.00	0.331	118.35
-21.3465	64.0530	5132	HE-24	-5.87	-60.94	-8.51	-67.34	1908.0	702.117	2763.9	-7.414	-64.683	7.20	0.585	116.90

TABLE 5: Stable isotopes values (ä) for the Nesjavellir wells in 1985 -1989 before production started (Sveinbj rnd–ttir, 1989)

Location	Well no.	Eastings	Northings	$\delta^{18}O$ g	$\delta^{18}O$ v	Steam ratio	$\delta^{18}O$	T_{sqp} (aC)	$\delta^{2}Hg$	$\delta^{2}Hv$	$\delta^{2}H$	T_{sqp} (aC)
95001	NV-1	-21.26683	64.10251	-6.600	2.750	0.950	-6.410	142.00	-79.000	-54.900	-77.800	112.00
95005	NG-5	-21.26049	64.10364	-7.750	-5.050	0.808	-6.280	137.50	-74.450	-69.100	-71.500	190.50
95006	NG-6	-21.27297	64.09665	-6.015	-3.955	0.378	-5.630	223.75	-75.000	-73.075	-74.830	211.25
95007	NG-7	-21.25743	64.10570	-8.265	-5.563	0.950	-6.585	189.25	-79.600	-73.675	-75.900	189.50
95008	NG-8	-21.27935	64.09556	-6.350	-2.600	0.950	-6.160	146.00	-63.200	-73.675	-62.800	181.00
95009	NG-9	-21.26881	64.09461	-6.696	-3.433	0.825	-6.220	173.38	-75.375	-64.925	-74.300	156.50
95010	NG-10	-21.25534	64.10032	-8.200	-5.700	0.393	-6.600	198.67	-80.000	-75.000	-76.930	193.00
95011	NJ-11	-21.26298	64.10735	-6.780	-4.210	0.898	-6.505	190.66	-74.925	-69.133	-74.325	190.30
95012	NJ-12	-21.28083	64.10386	-9.425	-6.841	0.390	-7.860	178.60	-77.950	-72.810	-74.916	192.33
95013	NJ-13	-21.26996	64.09879	-6.244	-4.020	0.840	-6.047	203.71	-75.900	-72.071	-75.285	198.85
95014	NJ-14	-21.27160	64.09048	-8.190	-5.160	0.420	-6.430	176.00	-79.200	-71.700	-74.900	188.00
95015	NJ-15	-21.25775	64.09675	-7.858	-5.538	0.525	-6.720	210.16	-74.450	-70.010	-72.300	196.40
95016	NJ-16	-21.25795	64.11096	-6.929	-4.259	0.771	-6.291	193.80	-76.160	-71.020	-74.966	191.40
95017	NJ-17	-21.28865	64.09969	10.108	-7.100	0.233	-7.803	175.00	-79.150	-70.250	-72.320	172.25
95018	NJ-18	-21.25694	64.12107	-10.97	-7.576	0.220	-8.324	158.00	-84.280	-72.975	-75.475	162.00

5.1.2 Chloride

Chloride is a conservative (non-reactive) constituent in a geothermal system. Once added to the fluid phase it remains there. Conservative components have not equilibrated in a thermodynamic sense. They are externally fixed by their sources of supply for the geothermal fluid (may dissolve from rock, but are not taken up by rock, i.e. external source). Their contents along the flow path are changed only by mixing and steam loss.

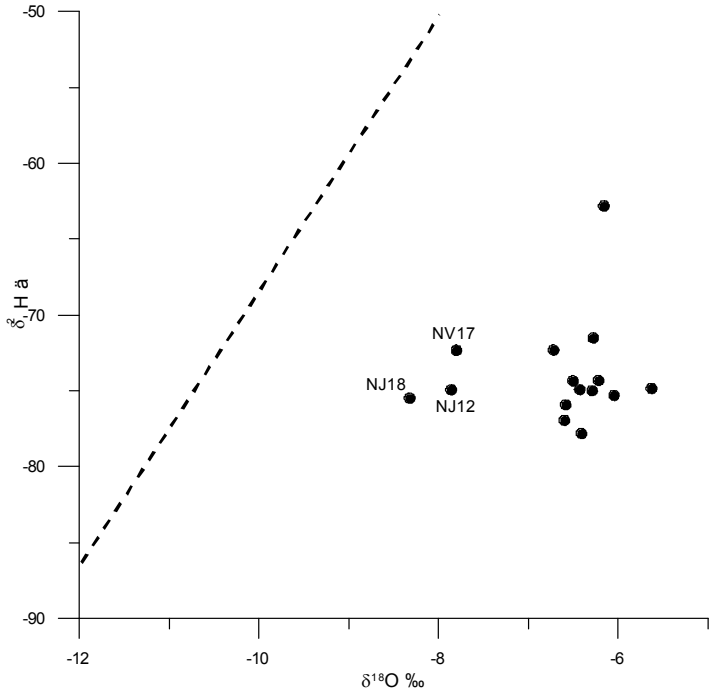

FIGURE 7: A graph showing δ^2H vs. $\delta^{18}O$ for the Nesjavellir wells, based on data from the 1980s

The chloride distribution during the pre-production years in the 1980s (Figure 9a) shows a distinct distribution with the highest values on the southeast side of the production field and the lowest values on the northern and western sides of the field. after production started the chloride concentration seems to have increased, as seen in Figure 9b which is based on data from 2000-2007, with high values being observed in the southern part of the field. The Nesjavellir reservoir shows important change from the initial Cl concentration as a consequence of the utilization. Initially, the Cl concentration in the wells closest to the young eruptive fissure was low, in some cases below 10 ppm, which is unusually low, but higher concentrations were found in the lower-enthalpy wells in the eastern part of the field. The recent increase in the Cl concentration may be due to an increase in the mineralisation of the fluids due to mixing or boiling, or perhaps mixing with waters from a different source with high chloride concentrations.

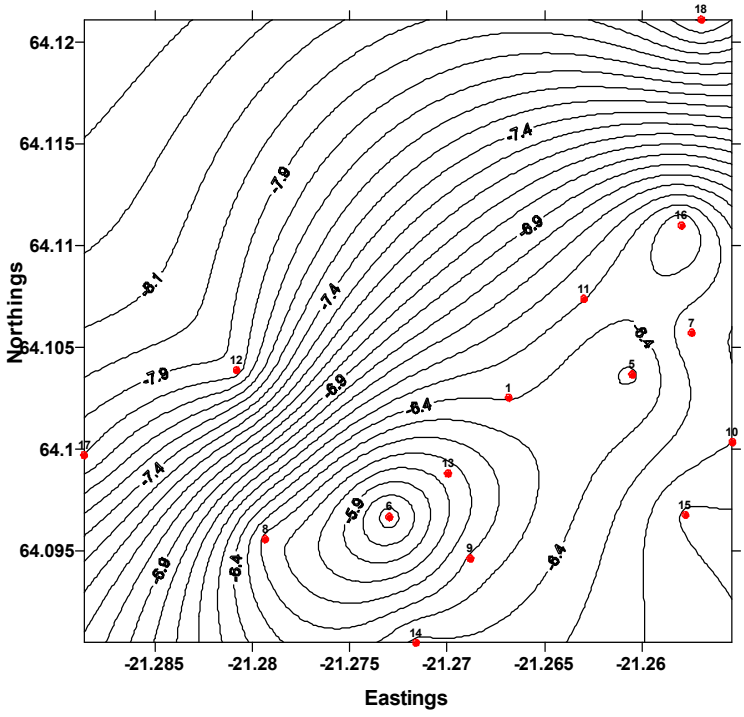

FIGURE 8: The distribution $\delta^{18}O$ in the Nesjavellir field in the 1980s

5.1.3 Enthalpy

In Figure 10 comparison is made between the enthalpy distribution based on the data from the 1980s (Figure 10a) and data from 2000-2007 (Figure 10b). The old data prior to exploitation shows the enthalpy distribution to be regular with the highest values of around 2100-2700 kJ/kg being observed along an axis in the central part of the field trending NE-SW. The same pattern is observed for the $\delta^{18}O$ distribution shown in Figure 8. This is the same direction as that of the fissure swarm which traverses Mt. Hengill into Lake Thingvalla-vatn. The data from 2000-2007 suggests a change in the distribution of the enthalpy (Figure 10b) where the enthalpy seems to be increasing outwards from the centre with a notable increase being observed to the northwest. This is a clear indication of an increase in temperature from the centre of the field outwards. As is to be expected when production is forced, the enthalpy rises with time. There is also a strong relationship between the enthalpy and the $\delta^{18}O$ isotopes distribution as indicated in Figure 11.

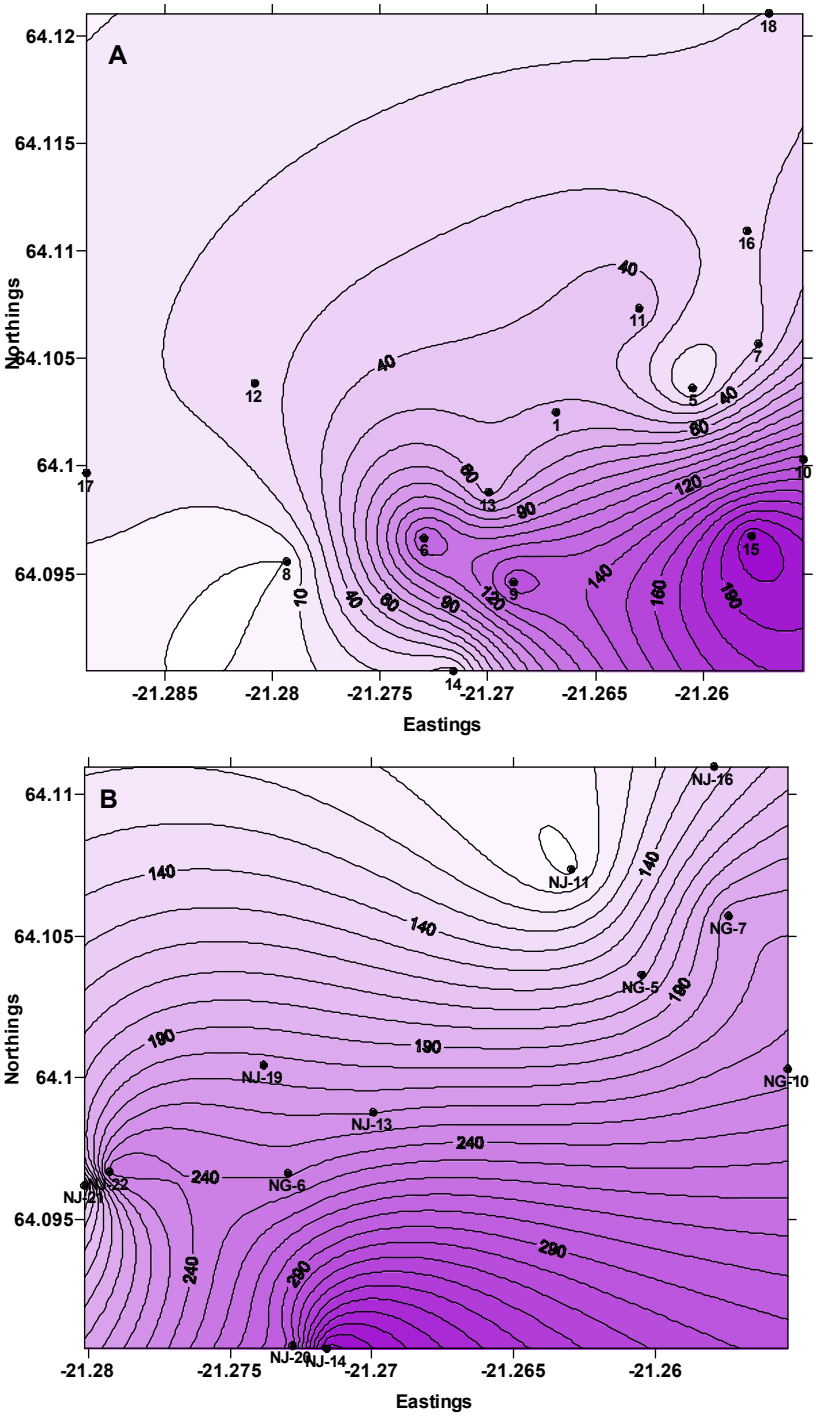

FIGURE 9: Distribution of Cl in the Nesjavellir field, based on data from a) 1980s; b) 2000-2007

5.1.4 CO_2 distribution

Figure 12 shows the distribution of CO_2 in the Nesjavellir field in the 1980s, before production started, and from 2000-2007. Before production, there is a CO_2 high in the southwestern part of the field. After some years of production, high CO_2 values are now observed in the northwest part. High gas concentrations are mainly due to flashing in the reservoir fluid (Björnsson, G., pers. comm.). This means that the response to production is increased flashing in the northwest part of the field.

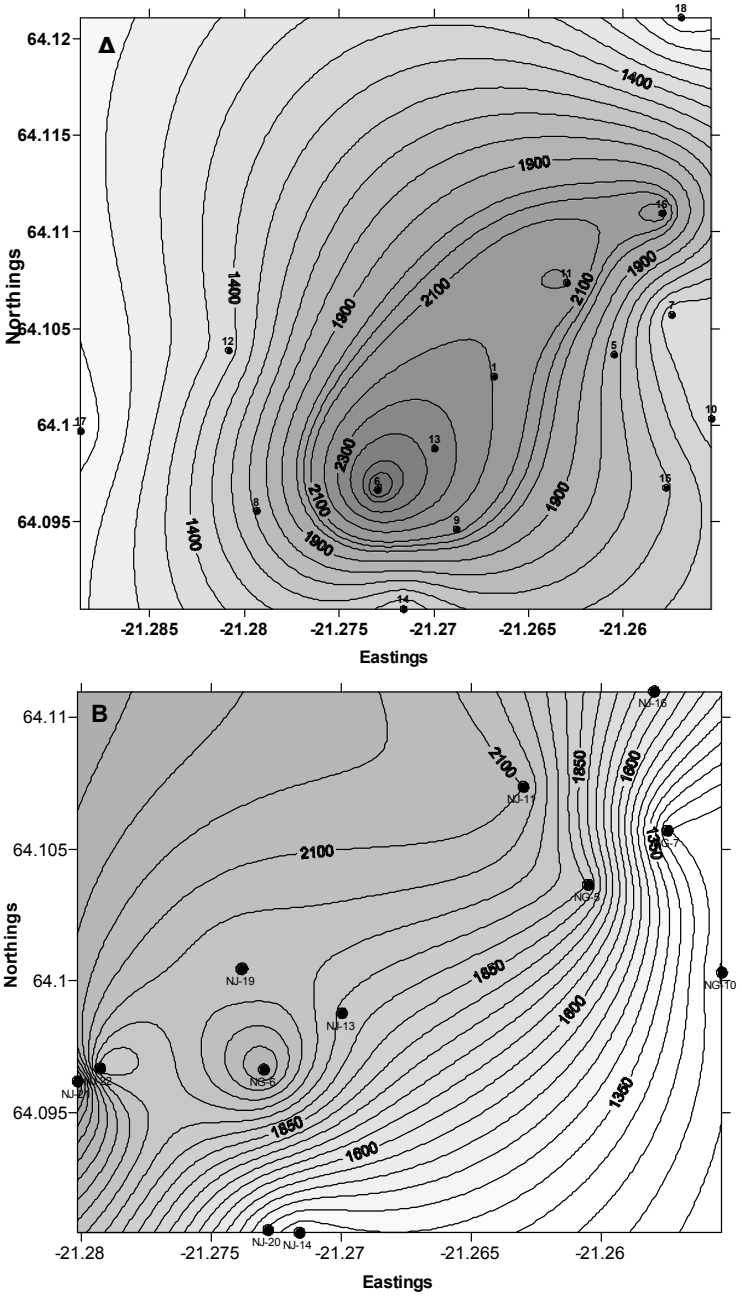

FIGURE 10: Distribution of enthalpy, *H* (kJ/kg), in the Nesjavellir field, based on data from a) 1980s and b) 2000-2007

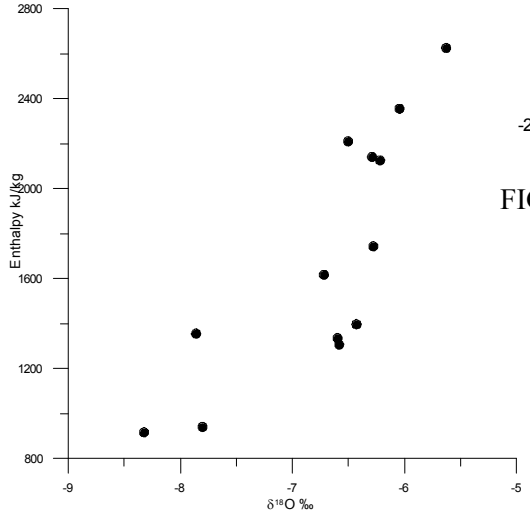

FIGURE 11: $\delta^{18}O$ vs. enthalpy for the Nesjavellir field for the data from the 1980s

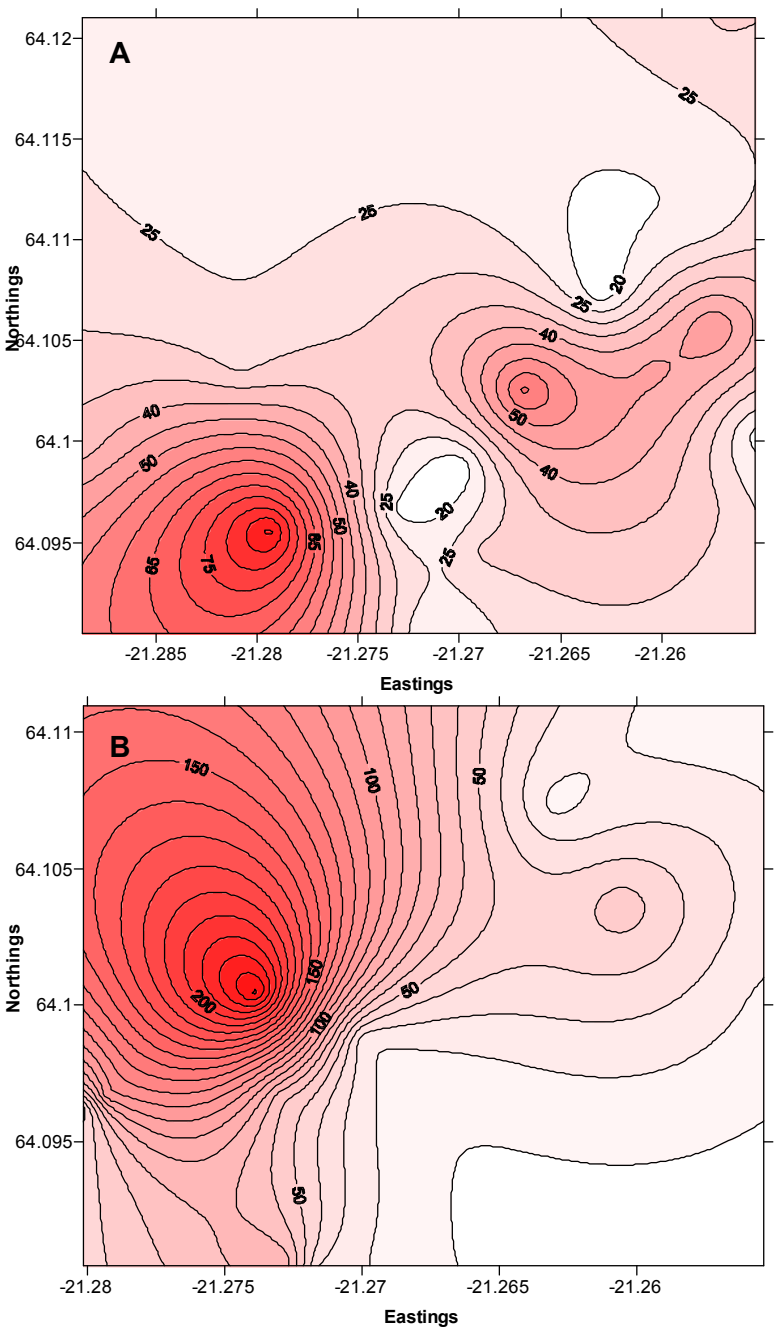

FIGURE 12: Distribution of CO_2 in the Nesjavellir field, based on data from a) 1980s and b) 2000-2007

5.1.5 Classification of the thermal fluid

The thermal waters in Nesjavellir field can be classified as partially equilibrated and mixed waters (Figure 13). There is not much change from the 1980s period, prior to production, to the period 2000-2007 when the field was in full production. Most samples fall in the temperature range of 240-300°C except for a few that fall above the fully equilibrated line, probably because of the removal of Mg from the waters.

The chemical composition of the fluids from the Nesjavellir wells in the period 2000-2007 shows that they can be classified as Cl-rich geothermal water (Figure 14), in contrast to the period in the 1980s where there is a scatter with most samples falling in the Cl-rich section but some within the HCO_3 rich section. The pH of most of the samples was in the range 8-9.

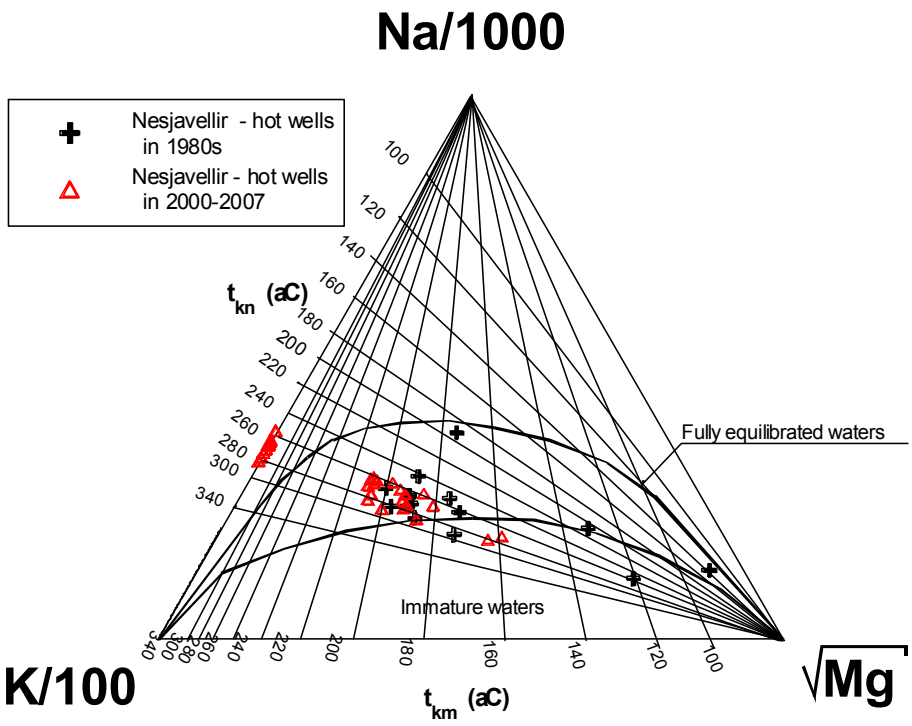

FIGURE 13: Na-K-Mg diagram for Nesjavellir water

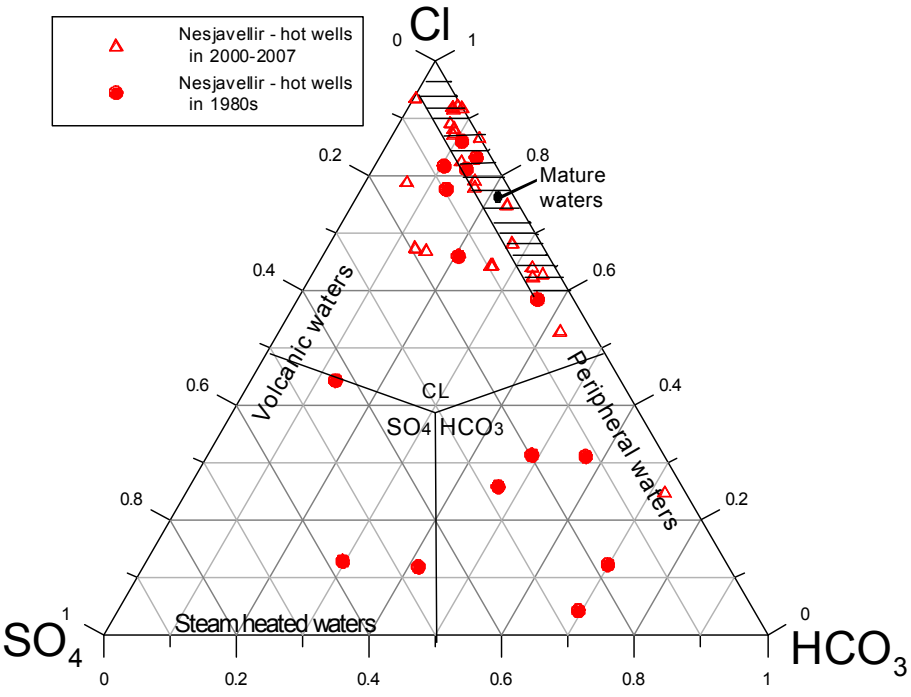

FIGURE 14: Cl-SO_4-HCO_3 diagram for Nesjavellir water, before and after production started

5.2 The Hellisheidi field

5.2.1 Stable isotopes

The samples for isotopes in the Hellisheidi field were collected in August 2007 comprising both condensate and steam. The results indicate that the isotope ratios for the deep circulating fluid range from -7.3‰ to -6.5‰ and -62‰ to -65‰ for $\delta^{18}O$ and $\delta^{2}H$, respectively. Figure 15 shows the distribution of $\delta^{18}O$ isotopes in samples collected in August 2007 from the wells in Hellisheidi. High values of $\delta^{18}O$ with a maximum value -6.5‰ are observed in the southwestern part of the study area and a minimum of -7.3‰ in the north. Wells HE-24 and HE-25 were producing from a steam cap, which means that their steam is much lighter in isotopes than steam from wells HE-7 and HE-17 which are two-phase.

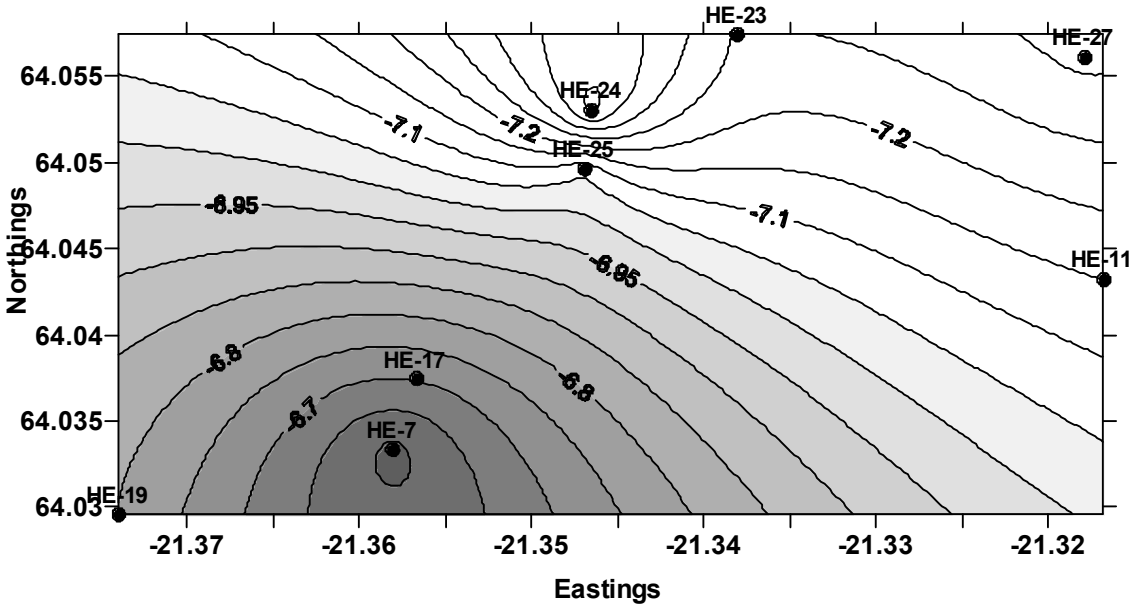

FIGURE 15: The $\delta^{18}O$ isotope distribution for the Hellisheidi field in 2007

Figure 16 shows that water from cold water wells in Hellisheidi (Ólafsson, M., pers. comm.) plots directly on the global meteoric water line and range in $\delta^{2}H$ from about -53‰ to -61‰. The geothermal waters show oxygen shift of about 2-3‰ and range in $\delta^{2}H$ between -2.0 and -65.0‰.

A linear relationship between $\delta^{18}O$ and Cl concentration, but not for $\delta^{2}H$ and Cl concentration, is observed for fluid from wells HE-7, 17, 19 and 24 (Figure 17a and b). The $\delta^{18}O$ ratios and the Cl concentrations in fluid from HE-7, 17 and 19 are relatively high, probably due to a long residence time resulting in significant water-rock interaction.

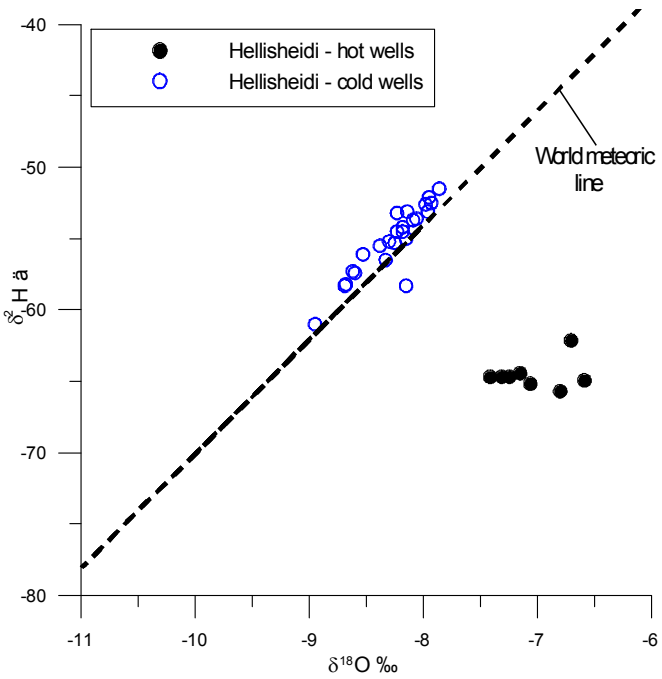

FIGURE 16: A graph showing $\delta^{2}H$ vs. $\delta^{18}O$ for Hellisheidi well waters

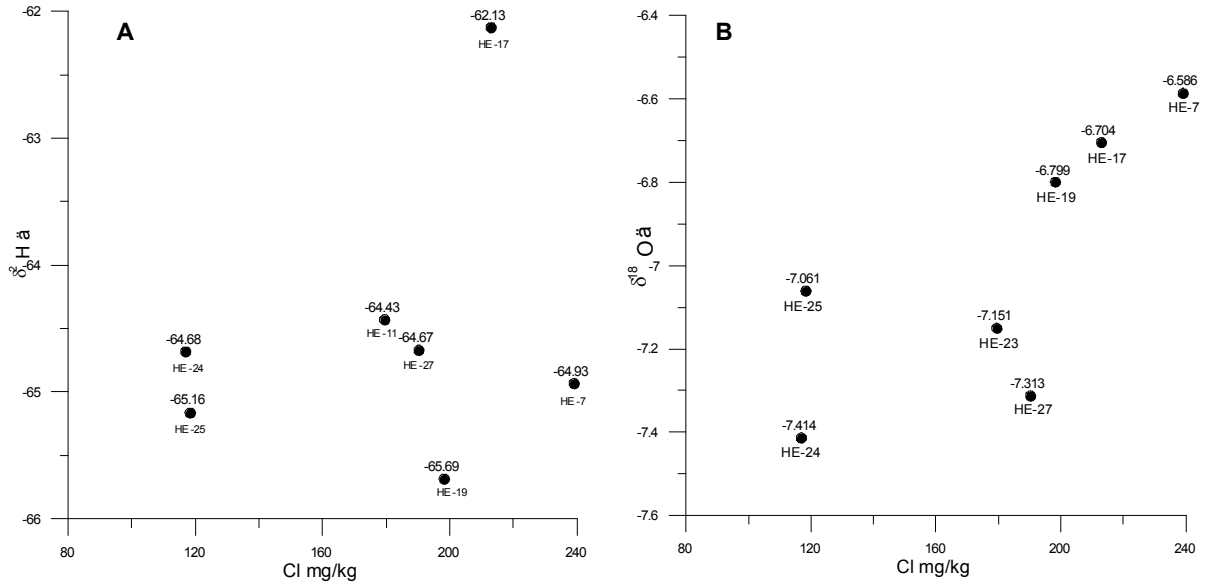

FIGURE 17: Graphs showing a) δ^2H vs. Cl and b) $\delta^{18}O$ vs. Cl, for the Hellisheidi geothermal wells

5.2.2 Chloride

Quite high chloride concentrations are observed in the Hellisheidi water with the highest values coinciding with the highest enthalpy and isotope values (Figure 18), due to boiling in the wells.

5.2.3 Enthalpy

High enthalpy values are generally observed in the Hellisheidi field with the highest values in the southwest and eastern parts (Figure 19). Figure 20 indicates that high enthalpy well fluids may have lower $\delta^{18}O$ values and vice versa.

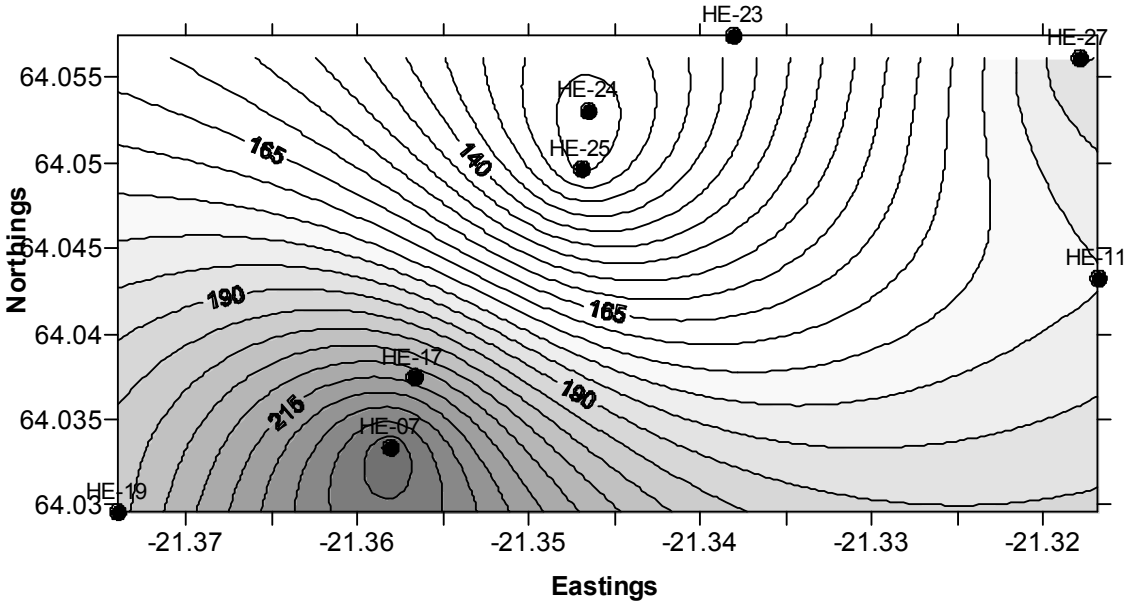

FIGURE 18: Distribution of Cl in the Hellisheidi field in 2000-2007

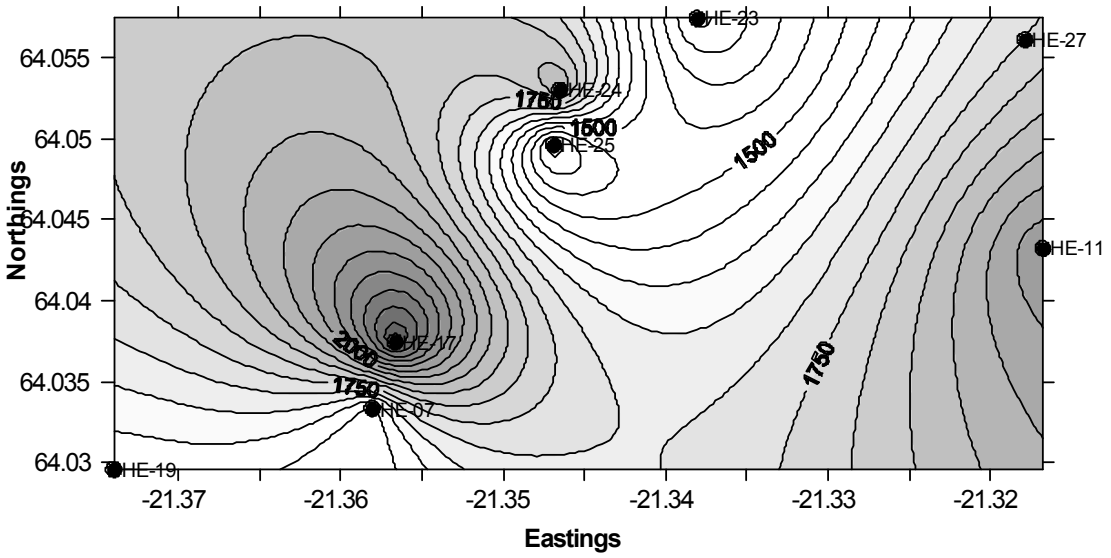

FIGURE 19: Enthalpy (kJ/kg) distribution in the Hellisheidi field in 2000-2007

5.2.4 CO_2 concentration

Figure 21 shows the CO_2 concentration in Hellisheidi fluid in 2000-2007. The highest values are seen in the northwest.

5.2.5 Classification of the thermal fluid

Most of the waters in this field fall are classified as partially equilibrated waters (Figure 22) with only a few samples above the fully equilibrated water line. That could be due to the removal of Mg ions (with the very low concentration of the ion probably due to boiling). All the cold well samples plot in the √Mg –corner of the diagram which means that these waters have not attained equilibrium. The cold waters are clearly peripheral waters while the hot waters are Cl-rich waters (Figure 23).

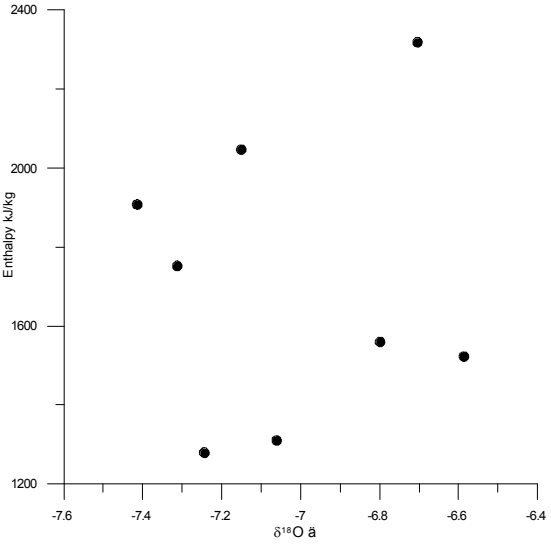

FIGURE 20: $\delta^{18}O$ vs. enthalpy for Hellisheidi fluid

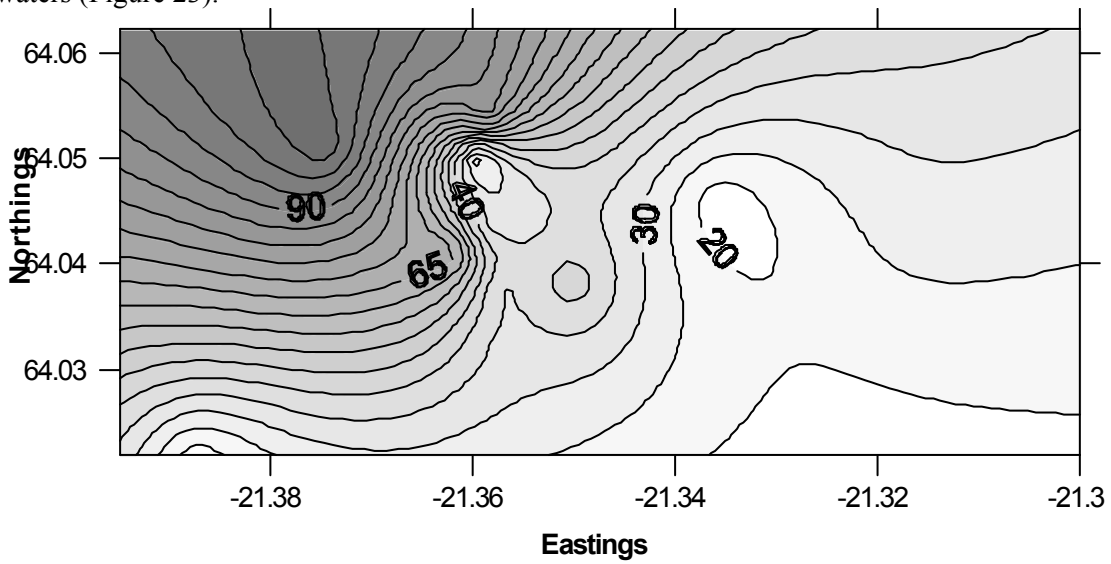

FIGURE 21: Distribution of CO_2 in Hellisheidi fluid 2000-2007

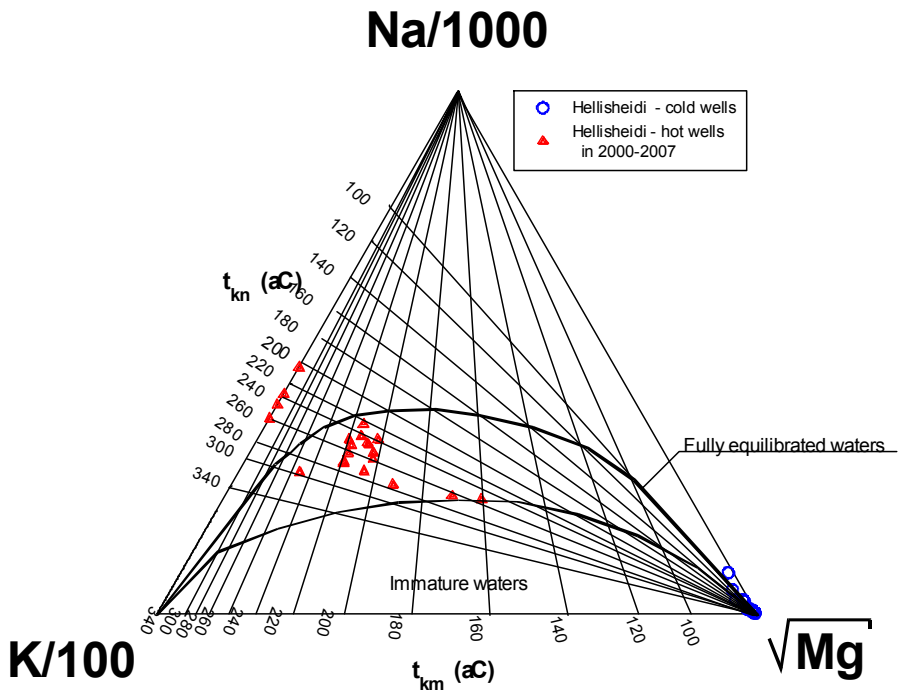

FIGURE 22: Na-K-Mg diagram for Hellisheidi waters

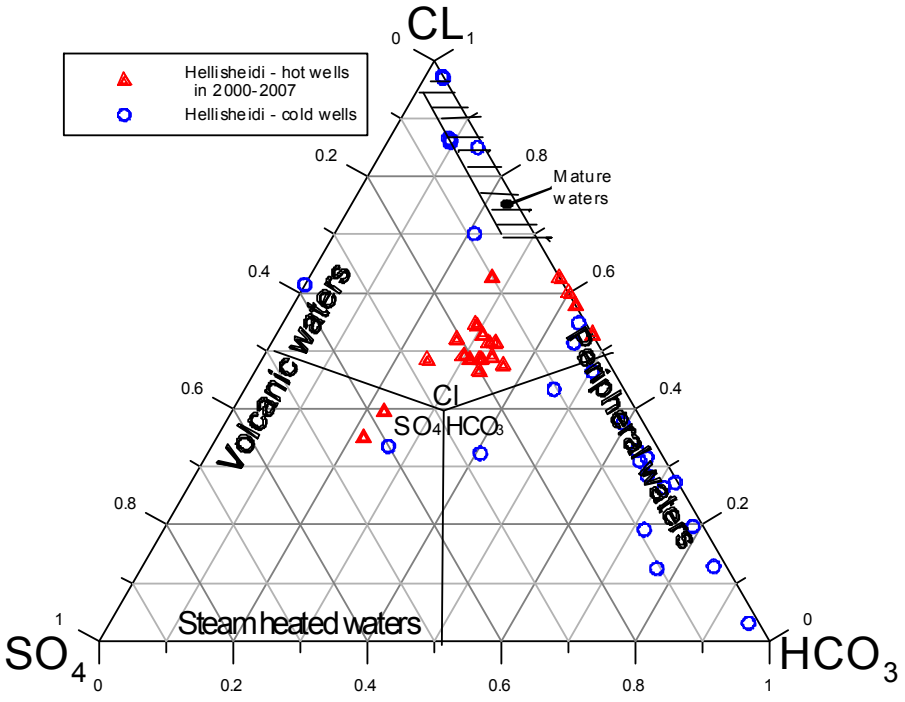

FIGURE 23: Cl-SO_4-HCO_3 diagram for Hellisheidi waters

5.2.6 Mineral saturation

Figure 24 shows a plot of the saturation index, *SI* = log *Q/K* for samples collected in December 2006 from well HE-17. The fluid is supersaturated with report to albite and adularia. Chalcedony and quartz seem to be in equilibrium at temperatures around 250°C. The enthalpy of this well is very high, 2533 kJ/kg, which means that more than 80% of the discharge is steam. Nevertheless, no best equilibrium temperatures can be found, probably owing to degassing or boiling, or some other processes such as precipitation of some minerals.

5.3 The Hveragerdi field – classification of the thermal fluids

Chemical data from the ÍSOR database for the Hveragerdi field has been plotted on a Na-K-Mg ternary diagram (Figure 25) and on a Cl-SO_4-HCO_3 diagram (Figure 26). Some fluids in the Hveragerdi wells can be classified as partially equilibrated waters and as mixed waters, but most samples plot above the fully equilibrated water line derived from Arnórsson et al. (1983), but are close to that of Giggenbach (1988). These data would fit Giggenbach's (1988) Na-K-Mg equilibrium curve for older and more acid rocks nicely, confirming the older age of the Hveragerdi system, also evident from the Cl-SO_4-HCO_3 diagram. The waters seem to have low temperatures with most of the samples in the range 100-140°C, with a few samples suggesting temperatures above 200°C (Figure 25). The temperature range 100-140°C implies an old system that is cooling down. The waters in Hveragerdi are probably mature Cl-type water, as indicated in Figure 26.

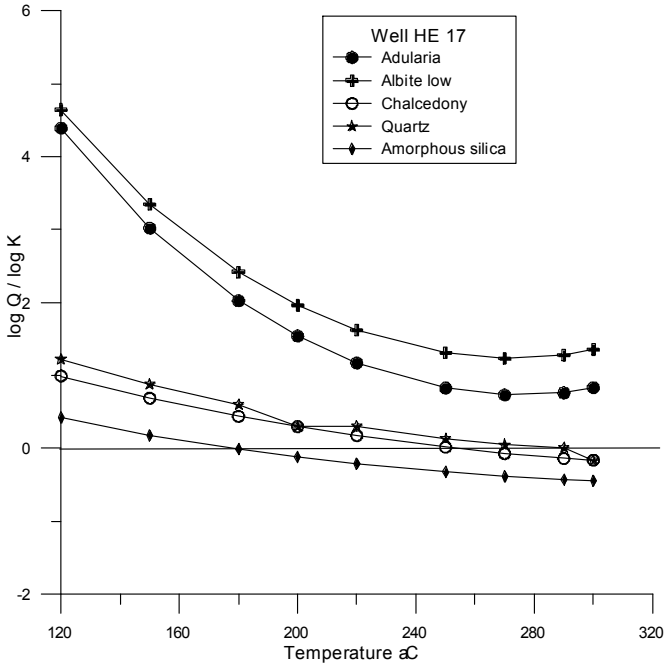

FIGURE 24: Graph showing a log Q/K vs. temperature for the Hellisheidi waters

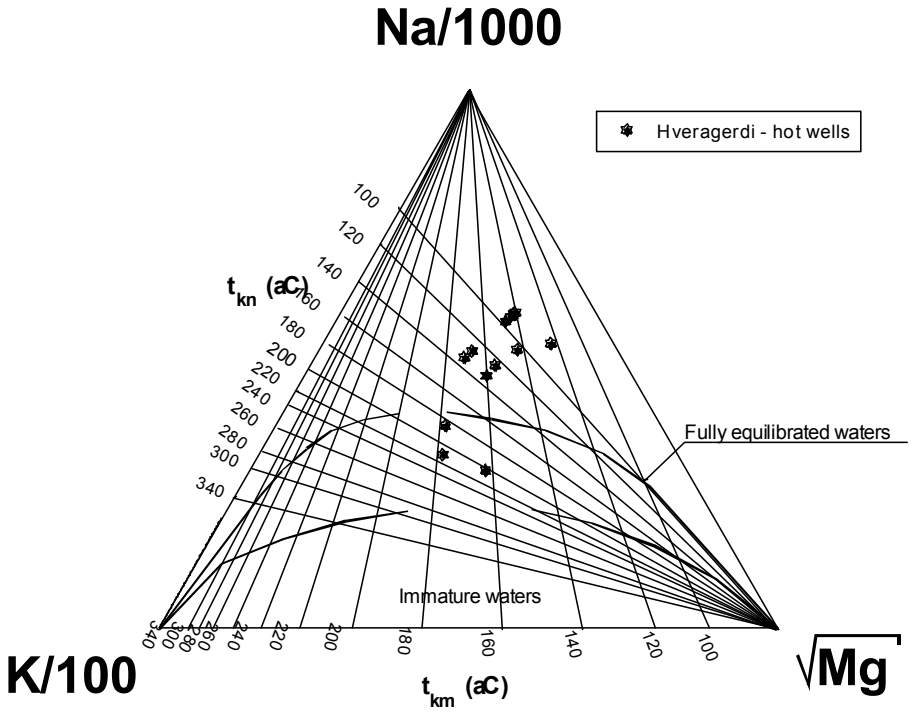

FIGURE 25: Na-K-Mg diagram for waters from Hveragerdi hot wells

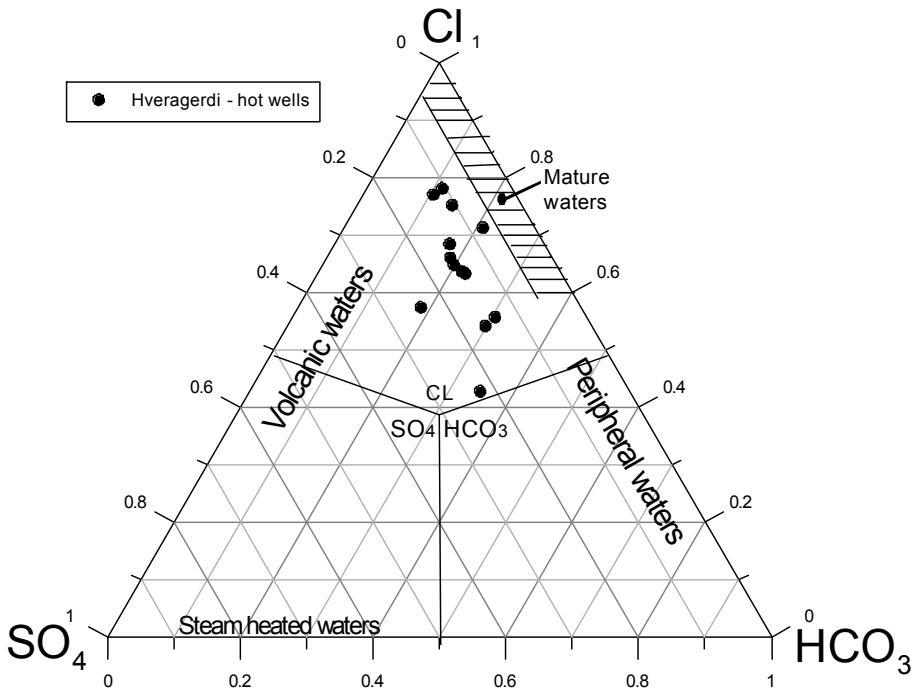

FIGURE 26: Cl-SO_4-HCO_3 diagram for waters from Hveragerdi hot wells

6. DISCUSSION

Figure 27 shows δ^2H plotted as a function of $\delta^{18}O$ for all the water samples from the three fields studied. The δ^2H of the thermal waters is in the range -62‰ to -78‰ and $\delta^{18}O$ ranges between -5.5‰ and -7.8‰. The figure shows that the thermal water deviates from the world meteoric water line in an agreement with the results of Sveinbjörnsdóttir and Johnsen (1992), who observed that the deviation of the Nesjavellir fluid from the meteoric line was due to an oxygen isotope exchange with the bedrock. This exchange is slow when T ≤200°C but at higher temperatures it is sharply accelerated. As basaltic rocks contain very little hydrogen, there is hardly any hydrogen isotope exchange between rock and water and, therefore, the deuterium value for thermal water still characterizes that of the original fluid. The δ^2H of the thermal waters in the Nesjavellir field is about 15-18‰ lighter than the local precipitation, but similar to precipitation that falls on the glacier Langjökull some 100 km to north of the Nesjavellir thermal area. This has been suggested to indicate that the geothermal water circulating the Nesjavellir field originates from the glacier Langjökull where the water percolates into the bedrock and flows

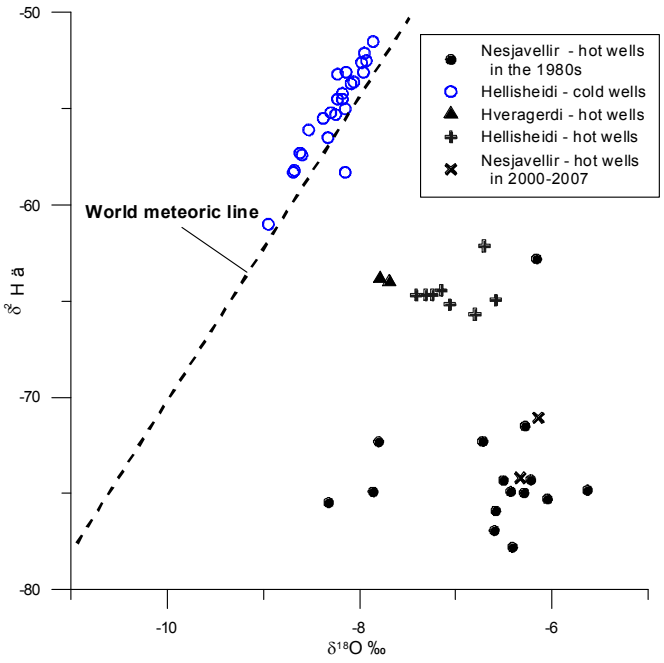

FIGURE 27: A graph showing δ^2H vs. $\delta^{18}O$ for all the available Hengill data

underground to the Nesjavellir field which is located southwest of Lake Thingvallavatn without mixing with water from the lake (Sveinbjörnsdóttir and Johnsen, 1992).

The δ^2H of local precipitation in Hellisheidi is estimated to be ca -60‰, which is slightly lighter than the estimate of the local precipitation in Hveragerdi (-56 ‰ (Árnason, 1976)) as Hveragerdi lies on lower grounds. Geothermal waters from Hellisheidi sampled and analysed for this study lie in the range from -62‰ to -65‰ in their δ^2H content, only about 1-5 ‰ lighter than the estimate of the local precipitation. It is therefore suggested that the origin of the thermal fluid circulating the Hellisheidi field is much more local than the water feeding the Nesjavellir system.

Water samples from drillholes and hot springs in Hveragerdi have a mean δ^2H value of -65.4 ‰ (Árnason, 1976), which is similar to the Hellisheidi thermal water. A conceptual model of the Hveragerdi high-temperature geothermal field based on water and gas chemistry and temperature logging data suggest that the geothermal fluid comes from the north and flows towards south along with temperature decrease caused by mixing processes with cold groundwater as well as conductive cooling (Geirsson and Arnórsson 1995, Sun, 1998). The δ^2H of the geothermal fluid fits well with this model.

While the deuterium ratios of the thermal fluids in Nesjavellir field suggest that the thermal waters originate as precipitation on the glacier Langjökull the thermal water in Hellisheidi is much closer to the local precipitation. It is however slightly more depleted in ^2H than the local precipitation suggesting either a slight mixture of the local precipitation with the light Nesjavellir fluid or that the water originate as has been suggested for the Hveragerdi thermal water, from the mountainous areas to the north of the field (e.g. Lyngdalsheidi). It should also be pointed out that the δ^2H content of the thermal fluids in Hellisheidi and Hveragerdi is very similar to that of the outlet of the Lake Thingvallavatn to the north of the fields (Sveinbjörnsdóttir and Johnsen, 1992).

The Na-K-Mg ternary diagram provides a clue as to whether geothermal water samples have been affected by mixing with groundwater. Figure 28 shows a Na-K-Mg diagram for all samples available from the Hengill area. Water samples that plot in the immature field of Figure 28 do not represent equilibrium conditions and are generally interpreted to have been affected by mixing with cold water, as Mg concentration decreases dramatically with increasing temperature (Fournier and Potter, 1979). Figure 28 shows that the cold Hellisheidi water samples plot in the Mg corner; as would be expected these waters have not matured. The Nesjavellir samples from 2000-2007 and the Hellisheidi samples follow a similar trend, with some samples plotting in the partially equilibrated water section and some in the fully equilibrated water section. These samples contain very little magnesium or no magnesium at all. The Hveragerdi waters plot

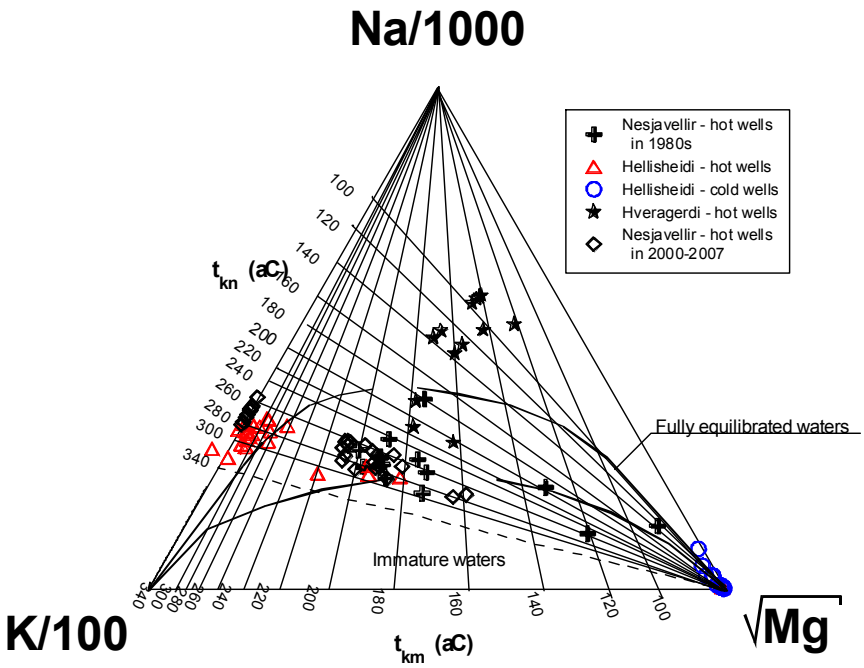

FIGURE 28: Na-K-Mg diagram for all samples available from the Hengill area

above the fully equilibrated waters line and most of the samples range in temperature from 100 to 140°C (Figure 28). The thermal fluids here are also Cl type fluids (Figures 26 and 29). This can be interpreted as a mature system that is cooling.

Some evidence indicates that the ascending hot water has mixed with cold water, such as:

- On the Na-K-Mg diagram (Figure 28) many samples from Nesjavellir, Hellisheidi and Hveragerdi plot in the area of mixed waters.
- A linear relationship can be inferred between Cl and B (boron) for samples from the Hellisheidi and Nesjavellir fields (Figure 30). Quite high Cl concentrations have been observed in both fields.

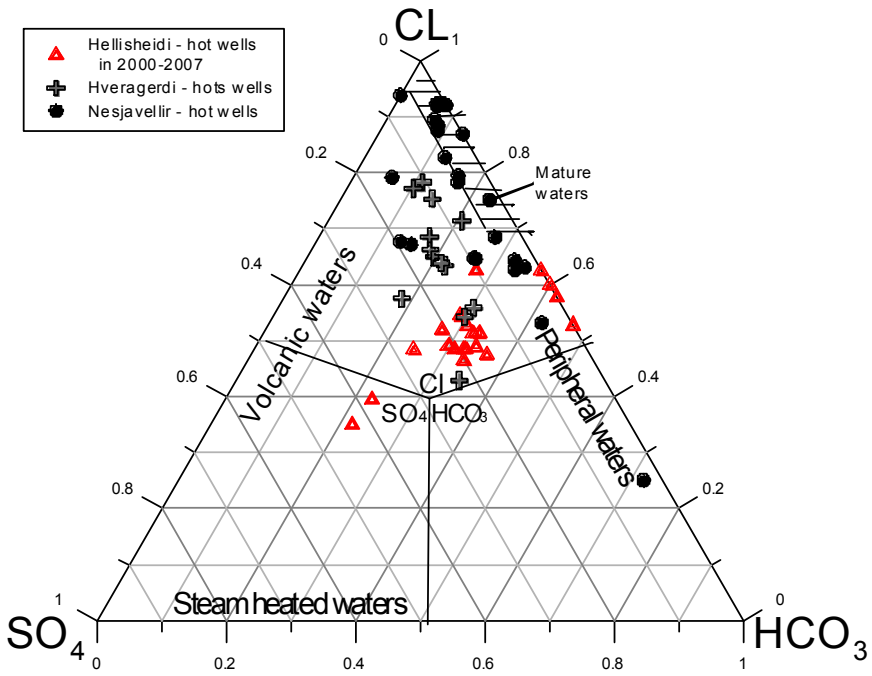

FIGURE 29: Cl-SO_4-HCO_3 diagram for all samples available from the Hengill area

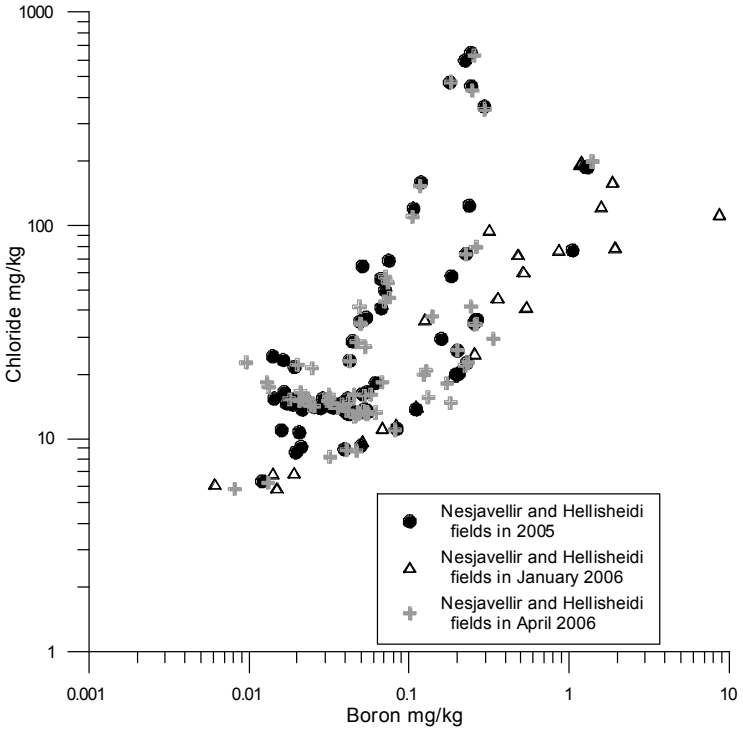

FIGURE 30: A graph showing boron vs. chloride for recent samples from the Nesjavellir and Hellisheidi fields

High CO_2 gas is due to reservoir flashing. The in-situ fluid has a small concentration of dissolved CO_2. When flashed, all these CO_2 molecules will boil into the steam phase and flow rapidly to the wells downstream. This explains the rise in CO_2. On the other hand, CO_2 levels decline again when the pressure stabilizes. This explains the change in CO_2 with time in the Nesjavellir.

Aquifer fluid compositions were calculated with the aid of the WATCH speciation program (Arnórsson et al., 1982; Bjarnason, 1994). Most of the wells in the Nesjavellir and Hellisheidi geothermal fields have excess enthalpy, i.e. the enthalpy of the discharged fluid is higher than that of steam saturated water at the respective aquifer temperature. This causes uncertainty as to how to obtain aquifer water composition from analysis of water and steam samples collected at the wellhead. Excess enthalpy may be a consequence of several processes (Arnórsson, 1991):

1) Partial segregation of the water and steam phases in the depressurization zone around the wells so that the water fraction is partially retained in the aquifer, while the steam flows into the wells.
2) Processes involving heat flow from the aquifer rock in the depressurization zone to the fluid flowing into the wells. The pressure drop causes boiling of the liquid phase which results in cooling and, hence, a positive temperature gradient is created between the aquifer rock and the flowing fluid.
3) Excess enthalpy could also be a reflection of a high steam fraction of the initial aquifer fluid.

Difficulties in evaluating the relative contribution of these boiling processes to the excess enthalpy of well discharges lead to uncertainties in how to calculate the chemical composition of the aquifer fluid from analytical data on water and steam samples collected at the wellhead, as illustrated in Figure 24.

The calculated quartz and chalcedony geothermometer values for the geothermal well waters indicate reservoir temperatures of 189-255°C. These values are lower than values calculated for cation geothermometers, probably due to the fast reaction rate of silica at high-temperatures. The Na-K-Ca and Na-K geothermometers give higher values for the wells, or 210-290°C. The gas geothermometers applied indicate temperatures of 232-295°C. However, the calculation of mineral saturation indices for the geothermal waters shows fluids from all the wells to be close to equilibrium at 245°C, and some degree of supersaturation with respect to amorphous silica, chalcedony and quartz.

Ívarsson (1998) used fumarole gas chemistry to estimate subsurface temperatures in this area. The highest temperatures were consistently found in the Nesjavellir field after production had started, while progressively lower temperatures were found in the Ölkelduháls and Hveragerdi fields. The gas chemistry suggests that the Nesjavellir and Ölkelduháls fields are not connected at depth.

Hellisheidi and Nesjavellir are sub-fields of the large Hengill geothermal system. Figure 31 shows reservoir temperature distribution in the Hengill area at 650 m b.s.l. based on the wells, and the conceptual reservoir model is shown in Figure 32 (Björnsson et al., 2006). An upflow zone of hot fluid resides beneath the summit of the Hengill volcano. A gradual rise in temperature is observed with depth in Nesjavellir, whereas temperatures are reversed at Hellisheidi; the reversal is explained by a lateral, cooler fluid recharge from the south. The ascending fluid then flows diagonally or laterally into both the Nesjavellir and the Hellisheidi fields (Björnsson et al., 2006).

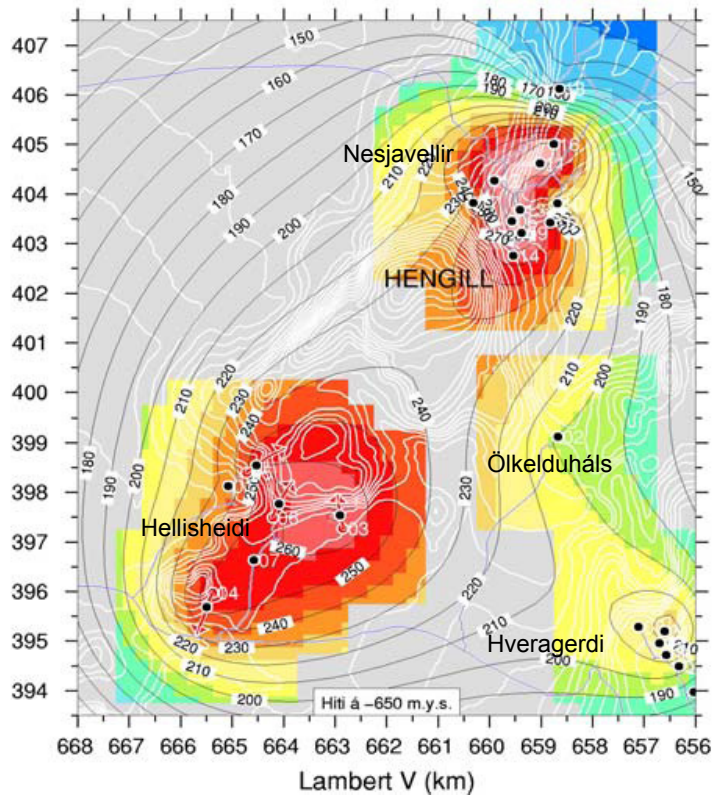

FIGURE 31: Reservoir temperature (°C) distribution in the Hengill area at 650 m b.s.l. based on chemical analyses from wells (Björnsson et al., 2006)

The isotopes, however, suggest a different origin for the thermal fluids in the two systems. The fluid circulating the Nesjavellir system comes from a distant source with δ^2H ranging from -72‰ to -78‰, being very similar to the local precipitation at the glacier Langjökull, some 100 km north of Nesjavellir. The δ^2H content of the Hellisheidi thermal

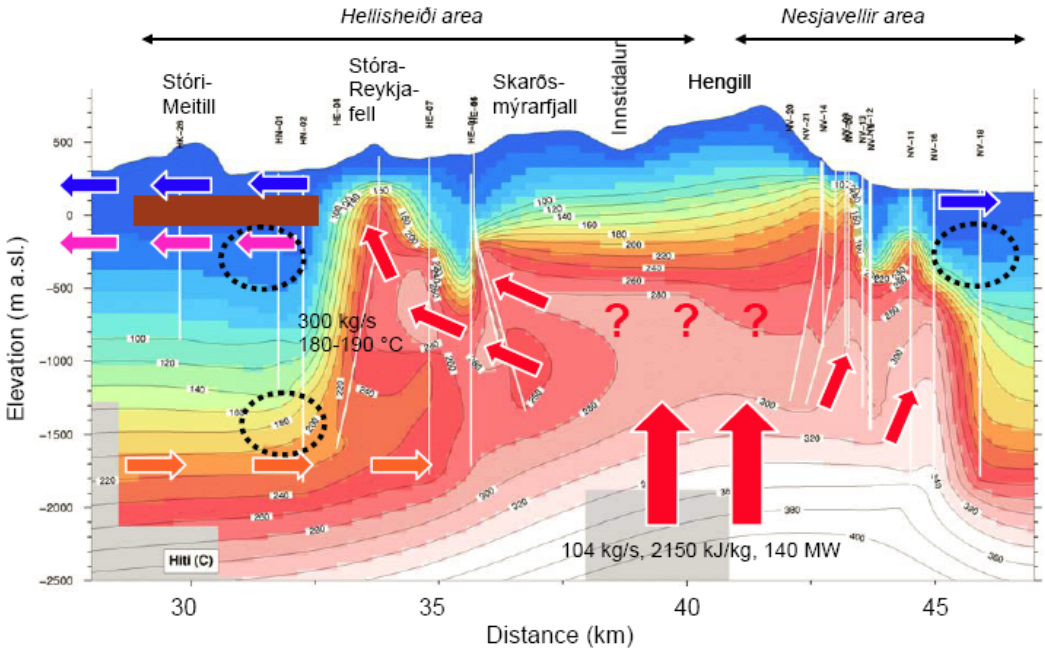

FIGURE 32: A SW-NE cross-section through the Hengill area including Hellisheidi and Nesjavellir, showing the expected temperature distribution (°C) and a conceptual reservoir model of the fluid flow (Björnsson et al., 2006)

fluid range between -62‰ and -66‰, only 1-5‰ more ^{2}H depleted than the local precipitation. Its origin is therefore more local; either it could be of local origin slightly mixed with the depleted Nesjavellir fluid or the fluid could originate from the mountainous areas to the north of the field as has been suggested for the Hveragerdi thermal fluid.

7. CONCLUSIONS

The main conclusions and recommendations can be summarized as follows:

- The Nesjavellir and Hellisheidi waters do not share the same origin. In Nesjavellir, the water originates from a distant source (the glacier Langjökull) whereas in Hellisheidi the water is more of a local origin. Either it could be of local origin slightly mixed with the ^{2}H depleted Nesjavellir fluid or the fluid could originate from the mountainous areas to the north of the field as has been suggested for the Hveragerdi thermal fluid.

- According to the deuterium isotope values, well HE-1 in Hellisheidi is closer in origin to the Nesjavellir thermal fluid than the fluid circulating in the rest of the Hellisheidi system.

- The Hellisheidi system is younger than the Nesjavellir system as is suggested by both the stable isotope ratios and by the chemistry of the thermal fluids ($Cl\text{-}SO_4\text{-}HCO_3$ diagram). At Nesjavellir, the fluid is richer in ^{18}O and chemically more mature than at Hellisheidi, due to more intense water-rock interaction

- There is an invasion of a different fluid with a high concentration of Cl in the Nesjavellir field. There is also increased boiling in the field, probably in general response to production.

- There is a pressure drop in both fields which causes boiling of the liquid phase, resulting in cooling. Thus, a positive temperature gradient is created between the aquifer rock and the

flowing fluid. Evidence of boiling can be seen in both the Nesjavellir and Hellisheidi fields by high CO_2 values. However, boiling is more pronounced in the Hellisheidi field as indicated by the Na-K-Mg diagram.

- The calculated quartz geothermometer for both fields indicate a conservative temperature range, between 189 and 255°C, but the Na-K geothermometers indicate higher temperatures beween 210 and 290°C.

- More samples should be collected for chemical and isotope analysis on a regular basis to better understand the Hengill geothermal systems/reservoirs.

ACKNOWLEDGEMENTS

My grateful thanks are due to many people without whose help this report would not have been produced. I would like to express my utmost appreciation to those who played a role and made possible my attendance at the Geothermal Training Programme, especially Dr. Simiyu of KenGen for nominating me for this course, to Dr. Ingvar B. Fridleifsson, Director, and Mr. Lúdvík S. Georgsson, Deputy Director, of the UNU Geothermal Training Programme, for recommending me for the UNU Fellowship and thus giving me the opportunity to participate in this special course, and also for their moral and technical support. I cannot forget Mrs. Dorthe H. Holm, Ms. Thórhildur Ísberg and Ms. Margrét T. Jónsdóttir for all the assistance during the course.

I would like to thank my supervisor, Prof. Árný Sveinbjörnsdóttir, for her support and guidance during my work on this project. Her critical review of the work as well as her encouragement, and enthusiasm are most appreciated. I would also like to express my deep gratitude to Dr. Halldór Ármannsson, whose helpful suggestions contributed significantly. My most sincere gratitude also goes to Mr. Gestur Gíslason of Reykjavik Energy for providing data as well as assisting in sample collection, and to Mr. Magnus Ólafsson for assisting with old data which was also very useful. The same can be said about all my lecturers in the UNU and ÍSOR who were always ready to assist, and to my new friends, the UNU-GTP 2007 Fellows. I thank all of you for your friendship and support. The University of Nairobi is acknowledged for granting me academic leave to pursue this course.

Finally, I would like give a very special thanks to my parents, siblings and friends who have been very supportive throughout my six months away from home.

REFERENCES

Ármannsson, H. and Ólafsson, M. 2000: *Collection of geothermal fluids for chemical analysis*. Iceland GeoSurvey, Reykjavík, report ISOR-2006/101, 17 pp.

Árnason, B., 1976: *Groundwater systems in Iceland traced by deuterium*. Soc. Sci. Islandica, 42, Reykjavík, 236 pp.

Árnason, K., Haraldsson, G.I., Johnsen, G.V., Thorbergsson, G., Hersir, G.P., Saemundsson, K., Georgsson, L.S., and Snorrason, S.P., 1986: *Nesjavellir, geological and geophysical surface exploration 1985.* Orkustofnun, Reykjavík, report OS-86014/JHD-02 (in Icelandic), 125 pp + maps.

Arnórsson, S., 1991: Geochemistry and geothermal resources in Iceland, In: D´Amore, F. (co-ordinator), *Applications of geochemistry in geothermal reservoir development.* UNITAR/UNDP publication, Rome, 145-196.

Arnórsson, S., (ed.), 2000: *Isotopic and chemical techniques in geothermal exploration, development and use. Sampling methods, data handling and interpretation.* International Atomic Energy Agency, Vienna, 351 pp.

Arnórsson, S., Gunnlaugsson, E., and Svavarsson, H., 1983: The chemistry of geothermal waters in Iceland. III. Chemical geothermometry in geothermal investigations. *Geochim. Cosmochim. Acta, 47,* 567-577.

Arnórsson, S., Sigurdsson, S., and Svavarsson, H., 1982: The chemistry of geothermal waters in Iceland I. Calculation of aqueous speciation from 0°C to 370°C. *Geochim. Cosmochim. Acta*, *46,* 1513-1532.

Bjarnason, J.Ö., 1994: *The speciation program WATCH, version 2.1.* Orkustofnun, Reykjavík, 7 pp.

Björnsson, A., Hersir, G.P., and Björnsson, G., 1986: The Hengill high-temperature area SW-Iceland: Regional geophysical survey. *Geoth. Res. Council, Transactions, 10,* 205-210.

Björnsson, G., Gunnlaugsson, E., and Hjartarson, A., 2006: Applying the Hengill geothermal reservoir model in power plant decision making and environmental impact studies. *Proceedings of the TOUGH symposium 2006, San Francisco, Ca,* 11 pp.

Bödvarsson, G., 1960: Exploration and exploitation of natural heat in Iceland. *Bull. Volcanol., 23,* 241-250.

Bödvarsson, G., 1961: Physical characteristics of natural heat resources in Iceland. *Jökull, 11,* 29-38.

Can, I., 2002: A new improved Na/K geothermometer by artificial neural networks. *Geothermics, 31,* 751-760.

Chiodini, G., Cioni, R., Guidi, M., and Marini, L., 1991: Chemical geothermometry and geobarometry in hydrothermal aqueous solutions: A theoretical investigation based on a mineral-solution equilibrium model. *Geochim. Cosmochim. Acta, 55*, 2709-2727.

Craig, H., 1961: Isotopic variations in meteoric waters. *Science, 133,* 1702-1703.

Craig, H., 1963: The isotopic geochemistry of water and carbon in geothermal areas. In: Tongiorgi, E. (ed.), *Nuclear geology on geothermal areas*. Consiglio Nazionale delle Ricerche, Laboratorio di Geologia Nucleare, Pisa, 17-53.

Ellis, A.J., and Mahon, W.A.J., 1977: *Chemistry and geothermal systems.* Academic Press, New York, 392 pp.

Ellis, A.J., and Wilson, S.H., 1960: The geochemistry of alkali metals ions in the Wairakei hydrothermal system. *N.Z.J. Geol.& Geophys., 3*, 593-617.

Fournier, R.O., 1977: Chemical geothermometers and mixing model for geothermal systems. *Geothermics, 5,* 41-50.

Fournier, R.O., 1979: A revised equation for Na-K geothermometer. *Geoth. Res. Council, Trans., 3,* 221-224.

Fournier, R.O, 1991: Water geothermometers applied to geothermal energy, In: D´Amore, F., (coordinator), *Application of geochemistry in geothermal reservoir development.* UNITAR-UNDP Publication, Rome, 37-69.

Fournier, R.O., and Potter, R.W. II, 1979: Magnesium correction to the Na-K-Ca geothermometer. *Geochim. Cosmochim. Acta, 43,* 1543-1550.

Fournier, R.O., and Potter, R.W., 1982: An equation correlating the solubility of quartz in water from 25° to 900°C at pressures up to 10,000 bars. *Geochim. Cosmochim. Acta, 46*, 1969-1973.

Fournier, R.O., and Rowe, J.J., 1962: The solubility of cristobalite along the three-phase curve, gas plus liquid plus cristobalite. *Am.Mineralogist 47***,** 897–902.

Fournier, R.O., and Truesdell, A.H., 1973: An empirical Na-K-Ca geothermometer for natural waters. *Geochim. Cosmochim. Acta*, *37*, 1255-1275.

Franzson, H., 1998: Reservoir geology of Nesjavellir high-temperature field in SW-Iceland *Proceedings of the 19th annual PNOC-EDC Geothermal Conference, Manila,* 13-20.

Geirsson K.,and Arnórssom, S., 1995: Conceptual model of the Hveragerdi geothermal reservoir based on chemical data. *Proceedings of the World Geothermal Congress 1995, Florence, Italy, 2,* 1251-1256.

Giggenbach, W.F., 1988: Geothermal solute equilibria Derivation of Na–K–Mg-Ca geoindicators. *Geochim. Cosmochim. Acta, 52*, 2749–2765.

Giggenbach, W.F., 1991: Chemical techniques in geothermal exploration. In: D'Amore, F. (Coordinator), *Application of geochemistry in geothermal reservoir development*. UNITAR/UNDP publication, Rome, 119-142.

Giggenbach, W.F., Gonfiantini, R., Jangi, B.L., and Truesdell, A.H., 1983: Isotopic and chemical composition of Parbati Valley geothermal discharges, NW Himalaya, India. *Geothermics, 12*, 199-222.

Gíslason, G., Ívarsson, G., Gunnlaugsson, E., Hjartarson, A., Björnsson, G., and Steingrímsson, B., 2005: Production monitoring as a tool for field development; A case history from the Nesjavellir field, Iceland. *Proceedings of the World Geothermal Congress 2005, Antalya, Turkey*, CD, 9 pp.

Gonfiantini, R., 1978: Standards for isotope measurements in manual compounds. *Nature, 271*, 534-536.

Gudmundsson, B.T., and Arnórsson, S., 2005: Secondary mineral-fluid equilibria in the Krafla and Námafjall geothermal systems, Iceland*. Applied Geochemistry, 20,* 1607-1625.

Gunnarsson, I. and Arnórsson S., 2000: Amorphous silica solubility and the thermodynamic properties of H_4SiO_4° in the range of 0° to 350°C at P_{sat}. *Geochim. Cosmochim. Acta, 64*, 2295-2307.

Gunnlaugsson, E., and Gíslason, G., 2005: Preparation for a new power plant in the Hengill geothermal area, Iceland. *Proceedings of the World Geothermal Congress 2005, Antalya, Turkey*, CD 10 pp.

Hartanto, D.B., 2005: Borehole geology and alteration mineralogy of well HE-11, Hellisheidi geothermal field, SW-Iceland. Report 8 in: *Geothermal Training in Iceland 2005*. UNU-GTP, Iceland, 251-264.

Ívarsson, G., 1998: Fumaroles gas geochemistry in estimating subsurface temperatures at Hengill in south-western Iceland. *Proceedings, of the 9th Symposium on Water-Rock Interaction, Balkema, Rotterdam,* 459-462.

Kristmannsdóttir, H., 1979: Alteration of basaltic rocks by hydrothermal activity at 100-300°C. In: Mortland, M.M., and Farmer, V.C. (editors), *International Clay Conference 1978*. Elsevier Scientific Publishing Co., Amsterdam, 359-367.

Morey, G.W., Fournier, R.O., and Rowe, J.J., 1962: The solubility of quartz in water in the temperature interval from 29 to 300°C. *Geochim. Cosmochim. Acta 26,* 1029-1043.

Natukunda, J.F., 2005: Geothermal exploration in eastern Ölkelduháls field, Hengill area, SW-Iceland. Report 14 in: *Geothermal Training in Iceland 2005.* UNU-GTP, Iceland, 247-264.

Nieva, D., and Nieva, R., 1987: Developments in geothermal energy in Mexico, part 12-A: Cationic composition geothermometer for prospection of geothermal resources. *Heat Recovery Systems and CHP, 7,* 243-258.

Nouraliee, J., 2000: Borehole geology and hydrothermal alteration of well NJ-20, Nesjavellir high-temperature area, SW-Iceland. Report 15 in: *Geothermal training in Iceland 2000.* UNU-GTP, Iceland, 303-330.

Pang, Z., and Ármannsson, H. (editors), 2006: *Analytical procedures and quality assurance for geothermal water chemistry*. UNU-GTP, Iceland, Report 1, 172 pp.

Paces, T. (editor), 1991: *Fluid sampling for geothermal prospecting*. UNITAR/UNDP publication, Rome, 94 pp.

Panichi, C., Celati, R., Noto, P., Squarci, P., Taffi, L., and Tongiorgi, E., 1974: Oxygen and hydrogen isotope studies of Larderello (Italy) geothermal system. *Isotope Techniques in Ground Water Hydrology, IAEA, 2,* 3-28.

Pendon, R.R., 2006. Borehole geology and hydrothermal alteration of well HE-22, Ölkelduháls field, Hengill area, SW-Iceland. Report 18 in: *Geothermal training in Iceland 2006.* UNU-GTP, Iceland, 357-390.

Pope, L.A., Hajash, A., and Popp, R.K., 1987: An experimental investigation of the quartz, Na-K, Na-K-Ca geothermometers and the effect of fluid composition. *J. Volcanol. Geotherm. Res., 31*, 151-161.

Saemundsson, K., 1967: *Vulkanismus und Tektonik des Hengill-Gebietes in Sudwest-Island*. Acta Nat. Isl., II-7 (in German), 195 pp.

Saemundsson, K., 1978: Fissure swarms and central volcanoes of the neovolcanic zones of Iceland. *Geol. J., Sp. Issue, 10,* 415-432.

Saemundsson, K., 1979: Outline of the geology of Iceland. *Jökull, 29,* 7-28.
Saemundson, K., 1995: *Geological map of the Hengill area, 1:25,000.* Orkustofnun, Reykjavík.

Sigmundsson, F., Einarsson, P., Rögnvaldsson, S.T., Foulger G.R., Hodgkinsson, K.M., and Thorbergsson, G., 1997: The 1994-1995 seismicity and deformation at the Hengill triple junction, Iceland: triggering of earthquakes by minor magma injection in a zone of horizontal shear stress. *J. Geophys. Res., 102 – B7,* 15151-15161.

Sigvaldason, G.E., 1963: Epidote and related minerals in two deep geothermal drill holes. Reykjavik and Hveragerdi, Iceland. *U.S. Geol. Surv. Prof. paper 450-E,* 77-79.

Sun Zhanxue, 1998: Geothermometry and chemical equilibria of geothermal fluds from Hveragerdi, SW-Iceland, and selected hot springs Jiangxi provice, SE-China. Report 14 in: *Geothermal training in Iceland 1998.* UNU-GTP, Iceland, 373-402.

Sveinbjörnsdóttir, Á.E., 1989: Stable isotope measurements on the thermal water at Nesjavellir and Mosfellssveit geothermal fields, Iceland. *Proceedings of the 6th Water Rock Interaction Symposium. Balkema, Rotterdam,* 137-149.

Sveinbjörnsdóttir, Á.E., and Johnsen, S.J., 1992: Stable isotope study of the Thingvallavatn area. Groundwater origin, age and evaporation models. *Oikos,64,*136-150.

Sveinbjörnsdóttir, Á.E., Johnsen, S., and Arnórsson, S., 1995: The use of stable isotopes of oxygen and hydrogen in geothermal studies in Iceland. *Proceedings of the World Geothermal Congress, 1995, Florence, Italy, 2,* 1043-1048.

Tole, M.P., Ármannsson, H., Pang Z., and Arnórsson, S., 1993: Fluid/mineral equilibrium calculations for geothermal fluids and chemical geothermometry. *Geothermics, 22*, 17–37.

Tonani, F., 1980: Some remarks on the application of geochemical techniques in geothermal exploration. *Proceedings of the Adv. Eur. Geoth. Res. 2nd Symposium, Strasbourg*, 428-443.

Truesdell, A.H., 1976: Summary of section III - geochemical techniques in exploration. *Proceedings of the 2nd U.N. Symposium on the Development and Use of Geothermal Resources, San Francisco, 1,* liii-lxxix.

Verma, M.P., 2000: Chemical thermodynamics of silica: a critique on its geothermometer, *Geothermics, 29*, 323-346.

Verma, S.P., and Santayo, E., 1997: New improved equations for Na/K, Na/Li and SiO_2 geothermometers by outlier detection and rejection. *J. Volcanol. Geotherm. Res., 79*, 9-23.